

Reply to Referee J. Cole

We thank the Referee for his comments that have all been taken into account and significantly improved the manuscript. A “bold” text copy of the manuscript (where all the minor changes and improvements with regard to the previous version, except the removed parts, are in red bold) is attached to this reply as a supplement.

Below are the replies to all the general points raised by the referee (referee’s points in italic and Authors’ replies in blue):

The description of events during the Caldera/Post-caldera evolution is confusing, largely because of differing names used. For example; the Cuicuilitic Member is variously called simply ‘Cuicuilitic’ (in some figures), Cuicuilitic member, Cuicuilitic de-posit, Cuicuilitic pyroclastics, Cuicuilitic rocks, and Cuicuilitic stage, with occasional reference to the mapping unit Qtc! There is no real description of this unit, which appears to be a key to understanding the evolution, but one assumes it is a Plinian airfall deposit, so perhaps ‘Cuiluilitic Pyroclastics’ is the best term to use. Perhaps a simple table within Section 2, showing stratigraphy would help, but using terminology consistent with the text and figures.

We thank the referee to this comment. We decided to use the term ‘Cuiluilitic Member’ throughout all the text to be consistent with the term used by [Dávila-Harris and Carrasco-Núñez, 2014] which provides a detailed description of this deposit. We also added a table (table 1 in the revised version of the manuscript) showing the stratigraphy described in section 2 and some details on the characteristics of the Cuicuilitic Member (lines 124-126 of the revised “bold” manuscript). The description of the evolution of the Los Humeros Volcanic Complex has been also partly rewritten and should be clearer now (lines 97-145 of the revised “bold” manuscript).

There are lots of redundant words in the text (e.g. Page 2, line 4: ‘On this regards’) and variability in spelling (e.g. Maztaloya in text; Maxtaloya in figures). There are a number of apparent typos (e.g. Cilinder for Cylinder in Fig. 2; Obsydian for Obsidian in Fig. 9). Figures in general do not relate well to the text, and labelling sometimes seems to differ from the caption (e.g. Figure 5e).

All the typos, redundant words have been corrected according to the referee suggestions (see the attached revised version of the manuscript).

Why are only experiments 4, 5 and 6 shown? Did experiments 1, 2 and 3 fail, or show different results not compatible with the conclusions? Why also are only the results of experiment 5 and 6, and not 4, shown in Figure 6, and which experiments are shown in Figure 7?

Some experiments failed for technical issues with the laser scanner or for the occurrence of an air bubble within the silicone. We decided to not include this information in the text because we believe is not useful for the reader. However, we agree with the reviewer that this may be confusing so we decided to label the experiments shown with consecutive numbers. Experiment 4 was not shown in figure 6 because replicates the same boundary conditions of experiment 5 and shows similar results ensuring the model reproducibility (now specified in the text, see lines 259-261 of the revised “bold” manuscript). Please note that we added two experiments to the dataset (see reply to referee E.Brothelande). We added the experiment number above each point in Figure 7 (now figure 8).

The reference to ‘graben formation’ should specify ‘apical graben formation’, otherwise there is a danger of confusion with regional tectonic features.

This has been changed. In accordance with the comment of referee 2 we changed the term “apical graben” with “apical depression”.

Figures are all generally useful, although 1 and 9 are very small and hard to read, and the use of red lettering in some darker figures (e.g. 5 and 6) is not recommended, as it is hard to read.

We separated Figure 1a (now Figure 1 in the revised copy of the manuscript) from Figures 1b and 1c (now figures 2a and 2b) to make them larger and easier to read. We also re-organized Figure 9 (now figure 10 in the revised manuscript) so that it should appear larger now. We changed the color lettering of figures 5 and 6 (now figures 6 and 7) to white.

I am not sure some photos add a great deal (e.g. Figure 4b and f).

We agree with the referee about figure 4b which may be redundant (now deleted in the revised version of the manuscript). Figure 4f does not exist thus the referee is probably referring to figure 5f. We agree with the referee and changed the photo of fig. 5f that better shows the alteration of the Cuicuiltic Member at Loma Blanca (now figure 6f in the revised manuscript).

The caption to Figure 8 is inadequate!

The caption has been rewritten (see Figure 9 and lines 652-656 of the revised “bold” manuscript).

In Figure 9c, why is the Los Humeros intrusion ‘projected’, if between 7.3– 3.8ka, and in the legend what is ‘Hydrothermalism’ (Alteration?)?

With the term “projected” we meant that the Loma Blanca and Los Humeros domes are not aligned with Arroyo Grande along the same plane as they appear in the schematic model (lines 677-678 of the revised “bold” manuscript). With ‘Hydrothermalism’ we were referring to hydrothermal activity (now corrected in figure 10 in the revised version of the manuscript).

The detailed replies to the specific comments raised by the referee, where a reply was requested, are listed below:

Line 146: motor?

This has been changed (line 188 of the revised “bold” manuscript).

Line 159: ??

We thank the referee for this comment. The sentence was wrong. Some calculated values of the dimensionless ratios Π in nature were wrong and have been now corrected (Table 3 in the revised version of the manuscript). Moreover, we added the natural values of the parameters listed in table 1 (now table 2 in revised version of the manuscript) used for the calculation of the Π . The sentence has been rewritten and should be clearer now (lines 200-202 of the revised “bold” manuscript).

Lines 165-170: Note different spelling of figures...

This has been corrected with “Maxtaloya” throughout all the text and figures.

Line 179: “Lineament”

We prefer to use the term “lineament” for the Las Papas scarp which indicates that no significant deformation and alteration is found at the outcrop scale (see lines 218-220 of the revised “bold manuscript) allowing it to be distinguished from the other scarps of the area (showing alteration and/or deformation).

Line 182: does this have a name?

The deposit can be attributed to the Xoxoctic Tuff. A brief description of this deposit has been added to the text (lines 118-119 of the revised “bold” manuscript) and to table 1.

Line 193: exposes?

This has been changed (lines 230 and 237 of the revised “bold” manuscript)

Line 214: Why 5 + 6 what happened to 1,2,3. Why not include 4?

See reply to the general comment above.

Lines 270-276: Needs rewording

The paragraph has been rewritten (lines 343-348 of the revised “bold” manuscript).

Figure 1: Maybe better to change color (yellow?) as it is hard to distinguish from normal faults.

This has been changed as suggested by the referee.

Figure 9: Obsidian. Why projected?

We changed with Obsidian. With “projected” we meant that the Loma Blanca and Los Humeros domes are not aligned with Arroyo Grande along the same plane as they appear in the schematic model. We better specified this in the figure caption (lines 677-678 of the revised “bold” manuscript).

Reply to Referee E. Brothelande

We thank the Referee for her comments that stimulated to expand and better explain the outcome of the analogue models. The results of the analogue models are now presented more clearly and benefit of additional data. The introduction has been rewritten and a subsection with the interpretation of the analogue modeling results has been added in the discussion. A “bold” text copy of the manuscript (where all the minor changes and improvements with regard to the previous version, except the removed parts, are in red bold) is attached to this reply as a supplement.

Below are the replies to all the general points raised by the referee (referee’s points in italic and Authors’ replies in blue):

(1). Introduction should be reworked to better present caldera resurgence

References are missing in the introduction. Important articles related to caldera resurgence should be cited at the beginning. Smith and Bailey (1968) and Lipman (1984) are two key literature review papers that should be referred to when defining resurgence and its main characteristics.

We added the references suggested by the referee in the introduction (lines 33-35 of the revised “bold” manuscript).

When it comes to the magmatic origin of resurgence, it is not a resolved question yet, as hydrothermal systems are also important sources of deformation in calderas and as different processes and timescales overlap in post-collapse caldera deformation. This complexity should be mentioned and a few arguments in favor of the magmatic origin should be given (such as large amplitudes and long timescales of the uplift, magmatic intrusions found in old eroded resurgent calderas).

We followed the referee’s suggestion documenting all the processes that are thought to trigger resurgence (lines 35-42 of the revised “bold” manuscript).

“It is attributed to the emplacement of silicic magma”. I have reasons to believe that resurgence also happens in basaltic environments even if it is not documented yet (article in preparation on a caldera in Galapagos). Additionally, resurgence is often associated with the injection of more primitive (then more mafic) magma (see references in a paper you cited: Brothelande et al., 2016, P.2, end of the first paragraph).

We changed the text specifying that resurgence is commonly attributed to the ascent of silicic magma but, though rare, may be also due to the ascent of more primitive magma as recently documented in Alcedo (lines 43-47 of the revised “bold” manuscript).

When mentioning uplift styles and rates of natural resurgence, give specific natural examples (and associated references).

This has been done (lines 61-68 of the revised “bold” manuscript).

A short description of the morphology of resurgent structures should be given, so the reader could be able to compare Los Potreros resurgent dome to other examples, and know if it has a typical or atypical morphology. Most resurgent domes are elongated and host one (or several) longitudinal graben at the top (See for instance Fig. 1 of Brothelande et al., 2016). Can circular domes can be considered as less common in nature?

We added a short description of the morphology of some examples of resurgent domes (lines 47-51 of the revised “bold” manuscript). Sub-circular domes have been reported at Long Valley (Hildreth et al., 2017), Cerro Galan (Folkes et al., 2011), Grizzly Peak (Fridrich et al., 1991) with both longitudinal graben (Long Valley) or concentric fault blocks (Grizzly Peak) at the top. Despite being less common, we show that the shape of the dome (i.e.

elliptical or sub-circular) and/or of the apical graben/depression (i.e. longitudinal or concentric) has no influence on the inferred depth of intrusion (see the revised Discussion section and analogue modeling results).

L. 53-55 - Confusing sentence: “with resurgence within the innermost...due to the uplift of a resurgence due to...”. Please reformulate. Additionally “commonly” seems incorrect in this context.

We changed “commonly” with “previously” and rewritten the sentence so that it should be clearer now (lines 75-78 of the revised “bold” manuscript).

(2). Analogue modelling should be revised

L. 143 : incorrect use of term “respectively”.

This has been deleted.

Figure 2 should be better designed: it does not show how the silicone intrudes the sand pack. Caption can be completed as well.

We have redrawn fig. 2 (now figure 3 in the revised manuscript) which now shows that the silicone intrudes the sand pack from its base and completed the caption (lines 588-590 of the revised “bold” manuscript).

I would not use the term graben to designate the crestal depression that develops at the apex of a circular tectonic dome: a graben is generally a depressed block of the crust bordered by parallel faults.

We changed the term “graben” with “apical depression” where necessary.

A very small number of experiments were conducted: 3. This is far to be enough to be representative and reliable. How are experiments 4 and 5 different in terms of initial conditions? It seems there is only two sets of different initial conditions.

We thank the reviewer for this comment. As now shown in table 3 we performed 5 experiments testing three different values of the overburden thickness ($T= 10, 30$ and 50 mm) and replicating some experiments to ensure their reproducibility and reliability (experiments 1 and 2 and experiments 3 and 4 now specified in the revised text, see lines 259-261 of the revised “bold” manuscript). Since no difference is observed in the replicated experiments, we show only the three representative ones for each value of T . Please note

that we changed the labeling of the experiments so that they appear numbered in series now (see also reply to referee J. Cole).

Two additional concerns arise from there:

The sand pack thickness T is considered as the only unknown variable. Unless it is properly justified, the source diameter D is also unknown, and should be varied. D is commonly considered as a variable in experiments, that show a high relevance of the T/D ratio.

We agree with the reviewer comment. One of the findings of our paper is that the linear relationship between the graben (or apical depression in our case) width and the overburden thickness found in Brothelande and Merle 2015 is confirmed for sub-circular sources thus we are interested to investigate resurgent domes. Therefore, testing different source diameters so that $T/D = 1$ is not useful for our purposes as we would have obtained resurgent blocks and no apical depression would have formed as shown by (Acocella et al., 2001). Despite it would be interesting to see if the tested relationship is affected by the source diameter (but still in the resurgent domes regime), we believe that the new findings of this paper are still interesting and stimulating for future experimental works on this topic.

The authors claim they evidence a linear relationship between L_g and T (L.257 – Fig. 7): how can a relationship be inferred from only two points?

With the new added experiments to the dataset, we believe that 5 experiments are enough to confirm the linear relationship between L_g and T for sub-circular domes.

I am very confused by the author's choice of model geometries. This manuscript present experiments of circular shaped domes with circular depressions in order to interpret an elongated dome with a longitudinal graben (Loma Blanca bulge). Why?

One of the aims of our paper is to test the validity of relationship found by Brothelande and Merle 2015 for circular domes. This is particularly useful for the Los Potreros case study showing both sub-circular (Arroyo Grande) and elliptical (Loma Blanca) bulges. Therefore, having demonstrated that the tested relationship is independent from the source eccentricity, we use our results to estimate the intrusion depth of the Loma Blanca bulge. More in general, we would like to stress that it is the basic deformation pattern which matters, which is independent of any elongation of the structure, which represents only a minor complication of the basic pattern (e.g. Roche et al., 2000).

Then, they rely on Brothelande and Merle (2015) to complete their results interpretation and T_t calculation. However, the geometry of models are different: Brothelande and Merle study elongated sources with linear grabens. Is this exactly comparable?

This is one of the new findings of our paper. Our results show that the theoretical equation for the calculation of T_t found in Brothelande and Merle 2015 with elliptical sources is still applicable for subcircular sources so it is independent from its eccentricity. Indeed, the percentage difference between T and T_t (see table 4) can be considered as a first order approximation of the source depth of resurgent domes, despite any eccentricity and shape of the apical extensional structures (i.e. linear grabens or sub-circular depressions).

On the other hand, previous analogue models of circular intrusion-related domes have been performed, some of which showing crestal depressions and radial extension patterns as in the authors experiments. However, they are very poorly referenced: Acocella et al., 2001; Walter and Troll, 2001; Marti et al., 1994; Galland et al., 2009, etc.

We warmly thank the reviewer for this comment and we apologize for the poor referencing. The suggested papers have been cited in a new subsection of the discussion (see the new subsection 5.1).

Please recall more clearly what were the main conclusions of resurgence analogue experiments, and how the new experiments in this manuscript were designed to complete these studies.

We have now better specified our conclusions and the rationale of the analogue experiments (lines 80-82; 84-86; 167-169; 279-298; 396-397 of the revised “bold” manuscript).

Sincerely,

The Corresponding Author

Stefano Urbani

Estimating the depth and evolution of intrusions at resurgent calderas: Los Humeros (Mexico)

Stefano Urbani¹, Guido Giordano^{1,2}, Federico Lucci¹, Federico Rossetti¹, Valerio Acocella¹, Gerardo Carrasco- Núñez³

¹Dipartimento di Scienze, Università degli Studi Roma Tre, L.go S.L. Murialdo 1, I-00146 Rome, Italy

²CNR - IDPA c/o Università degli Studi di Milano, Via Luigi Mangiagalli, 34, 20133 Milano

³Centro de Geociencias, Universidad Nacional Autónoma de México, Campus UNAM Juriquilla, 76100, Queretaro, Mexico

Correspondence to: Stefano Urbani (stefano.urban@uniroma3.it)

Abstract. Resurgent calderas represent a target with high potential for geothermal exploration, as they are associated with the shallow emplacement of magma, resulting in a widespread and long lasting hydrothermal activity. Therefore, evaluating the thermal potential of resurgent calderas may provide important insights for geothermal exploitation. Resurgence is classically attributed to the uplift of a block or dome resulting from the inflation of the collapse-forming magma chamber due to the intrusion of new magma. The Los Humeros volcanic complex (LHVC; Mexico), consisting of two nested calderas (the outer Los Humeros and the inner, resurgent, Los Potreros), represents an area of high interest for geothermal exploration to optimize the current exploitation of the active geothermal field. Here we aim at better define the characteristics of the resurgence in Los Potreros, by integrating field work with analogue models, evaluating the spatio-temporal evolution of the deformation and the depth and extent of the intrusions responsible for the resurgence and which may represent also the local heat source(s).

Structural field analysis and geological mapping show that Los Potreros area is characterized by several lava domes and cryptodomes (with normal faulting at the top) that suggest multiple deformation sources localized in narrow areas.

The analogue experiments simulate the deformation pattern observed in the field, consisting of magma intrusions pushing a domed area with apical **depression**. To define the possible depth of the intrusion responsible for the observed surface deformations, we apply **tested** established relations **for elliptical sources** to our experiments **with sub-circular sources**.

We found that these relations **are independent from the source and surface dome eccentricity and** suggest that the magmatic sources responsible for the deformation **in Los Potreros are** present at very shallow depths (hundreds of meters), which is in agreement with the well data and field observations. We therefore propose that the recent deformation at LHVC is not a classical resurgence associated with the bulk inflation of a deep magma reservoir; rather this is related to the ascent of shallow (<1 km) multiple magma bodies. A similar multiple source model of the subsurface structure has been also proposed for other calderas with an active geothermal system (Usu volcano, Japan) suggesting that the model proposed may have a wider applicability.

1 Introduction

Caldera resurgence consists of the **post-collapse** uplift of part of the caldera floor. **Resurgence has been described in several calderas worldwide (Smith and Bailey, 1968; Elston, 1984; Lipman, 1984 and references therein), representing a frequent step in caldera evolution. Several mechanisms have been invoked to trigger resurgence, including the pressurization of the hydrothermal system (Moretti et al., 2018), regional earthquakes (Walter et al., 2009), and magmatic intrusion (Kennedy et al. 2012). Discriminating the contributions to the observed uplift of each of these mechanisms is often challenging (Acocella, 2014). However, despite the possible hydrothermal and tectonic contributions, field observations in eroded resurgent calderas (e.g. Tomochic, Swanson and McDowell,**

1985; Kutcharo, Goto and McPhie 2018; Turkey Creek, Du Bray and Pallister, 1999) coupled with the long timescale of the uplift of the caldera floor (from tens to thousands years), suggest that the intrusion of magmatic bodies is the prevalent mechanism for resurgence.

Resurgence is commonly attributed to the emplacement of silicic magmas at different depth levels under limited viscosity contrasts with regard to the previously emplaced magma (Marsh, 1984; Galetto et al., 2017). However, though rare, resurgence may be also triggered by the injection of more primitive magma (Morán-Zenteno et al., 2004; Kennedy et al., 2012) or by the emplacement of basaltic sills, as recently documented at the Alcedo caldera (Galapagos; Galetto et al., 2019). The shape of the intracaldera resurgent structures is variable, being characterized by elliptical domes with longitudinal graben(s) at the top (e.g. Toba; De Silva et al., 2015; Snowdonia, Beavon, 1980; Timber Mountain, Christiansen et al., 1977) or, less commonly, by sub-circular domes (e.g. Cerro Galan, Folkes et al., 2011; Long Valley, Hildreth et al., 2017; Grizzly Peak, Fridrich et al., 1991) with both longitudinal grabens (Long Valley) or concentric fault blocks (Grizzly Peak) at their top.

Whatever is the shape, resurgence is often associated with hydrothermal and ore forming processes, since the circulation pattern and temperature gradients of geothermal fluids are structurally-controlled by the space-time distribution of faults and fractures and by the depth and shape of the magmatic sources (e.g. Guillou Frottier et al., 2000; Prinbow et al., 2003; Stix et al., 2003; Mueller et al., 2009). Therefore, the characterisation of the magma that drives resurgence (location, depth and size) and of the factors controlling the release of the heat (permeability, fracture patterns, and fluid flow) have important implications for the exploration and exploitation of renewable geothermal energy resources. In particular, the estimation of the location, depth and geometry of the magmatic sources is crucial to define the geothermal and mineral potential of resurgent calderas, allowing an economically sustainable exploration and exploitation of their resulted natural resources.

The depth and size of the magmatic sources influences the deformation style of the resurgence at surface (Acocella et al., 2001). Deep sources (i.e. depth/diameter ratio ~ 1 assuming a spherical source) are associated to resurgent blocks (e.g. Ischia and Pantelleria, Acocella and Funiciello, 1999; Catalano et al., 2009), whereas shallower sources (i.e. depth/diameter ratio ~ 0.4) to resurgent domes (e.g. Valles and Yenkahe, Kennedy et al., 2012; Brothelande et al., 2016). Moreover, uplift rates may change by one order of magnitude from ~ 1 to ~ 10 cm per year (e.g. Yellowstone and Iwo Jima, Chang et al., 2007; Ueda et al., 2018). Nevertheless, despite showing different uplift styles and rates, these natural examples share a common feature that is a coherent uplift of the caldera floor.

This scenario differs from the occurrence of deformation patterns characterized by the widespread and delocalized uplift of several minor portions of the caldera floor, due to lava domes and/or cryptodomes, as observed at Usu volcano (Japan, Matsumoto and Nakagawa, 2010; Tomya et al., 2010). A different depth and extent of the responsible source(s) and, consequently, a different subsurface structure of the volcano is therefore suggested. A better assessment of the subsurface structure in such cases has crucial implications for geothermal exploration in order to maximize the geothermal production.

The Los Humeros Volcanic Complex (LHVC, Mexico) is an important geothermal target area, consisting of two nested calderas: Los Humeros (the outer, larger and older one) and Los Potreros (the inner, smaller and younger one) (Fig. 1). The latter is characterized by the resurgence of its floor, which was previously interpreted as due to uplift processes related to the inflation of a several km deep magma chamber (Norini et al., 2015, 2019).

This paper aims at (1) evaluating the depth of the intrusion(s) responsible for the uplift in the LHVC area; (2) explain the spatio-temporal evolution of the observed deformation of the caldera floor and (3) test the validity of the linear relationship between the surface deformation structures and depth of elliptical sources (Brothelande and Merle

2015) for sub-circular sources. To achieve **these** goals, we integrate results from structural field investigations carried out within the Los Potreros caldera with those derived from analogue experiments specifically designed to constrain the depth of the deformation source(s) in volcanic caldera environments. **The obtained results show that: (1) the relation between the source depth and surface deformation structures is independent from the source eccentricity; (2) the LHVC is characterized by** discontinuous and small-scale (**areal extent** $\sim 1 \text{ km}^2$) surface deformations generated from multiple and shallow-**emplaced** ($< 1 \text{ km}$ **depth**) magmatic bodies. These results should be taken into account for **the** planning **of** future geothermal operations at the LHVC and in other calderas showing similar surface deformation.

2 Geological-structural setting

LHVC is located at the eastern termination of the Trans Mexican Volcanic Belt (TMVB, see inset in Fig. 1). The TMVB is the largest Neogene volcanic arc in Mexico ($\sim 1000 \text{ km}$ long and up to $\sim 300 \text{ km}$ wide), **commonly associated with** the subduction of the Cocos and Rivera plates beneath the North American plate along the Middle American trench (Ferrari et al., 2012, and references therein). The LHVC consists of two nested calderas formed during the Pleistocene: the outer $18 \times 16 \text{ km}$ Los Humeros caldera and the inner $10 \times 8 \text{ km}$ Los Potreros caldera (Fig. 1, Ferriz and Mahood, 1984; Norini et al., 2015; Carrasco-Núñez et al., 2017b).

Based on updated stratigraphic and geochronological information, the evolution of the LHVC can be divided **into** three **main eruptive** stages (**Table 1**, Carrasco-Núñez et al., 2017b, 2018). Pre-caldera volcanism extended between ca. 700 and 164 ka (U-Th and $^{39}\text{Ar}/^{40}\text{Ar}$ datings **in** Carrasco-Núñez et al., 2018), showing evidence for an extended building phase leading to the establishment of the large volume rhyolitic reservoir, **which fed several lava domes erupted to the western border of the Los Humeros Caldera. A** Caldera stage started at ca. 164 ka (U-Th and $^{39}\text{Ar}/^{40}\text{Ar}$ ages, Carrasco-Núñez et al., 2018), with the eruption of the 115 km^3 Xaltipan ignimbrite that triggered the collapse of the Los Humeros caldera. **This was followed by a Plinian eruptive episodic sequence, characterized by the emplacement of several rhyodacitic pumice fallout layers grouped as the Faby Tuff (Ferriz and Mahood, 1984). The Caldera stage** ended with the eruption of the 15 km^3 Zaragoza rhyodacite-andesite ignimbrite at $69 \pm 16 \text{ ka}$ ($^{39}\text{Ar}/^{40}\text{Ar}$ ages, Carrasco-Núñez et al., 2018) associated with the collapse of the nested Los Potreros caldera.

A post-caldera stage ($< 69 \text{ ka}$) is interpreted by Carrasco-Núñez et al. (2018) **as composed by two main eruptive phases: (i) a late Pleistocene resurgent phase, characterized by the emplacement of silica-rich small domes and disperse explosive activity within Los Potreros caldera,** followed by **(ii) Holocene basaltic to trachytic monogenetic, intra-caldera and at the caldera-rim,** volcanism. This **eruptive behaviour indicates a change in the** configuration of the magmatic plumbing system **with respect to the early caldera stage of Los Humeros, which has been referred to** an unique, large and homogenized magma reservoir (e.g. Ferriz and Mahood, 1984; Verma, 1985). **It is instead** in favour of a heterogeneous multi-layered system vertically distributed in the crust, with a deep (ca. 30 km **depth**) basaltic reservoir feeding progressively shallower and smaller distinct stagnation layers, pockets and batches up to very shallow conditions (ca. 3 km) (Lucci et al., under review).

During the early resurgent phase of the post-caldera stage, rhyolitic domes were emplaced along the northern rim of the Los Humeros caldera **and within the caldera at $44.8 \pm 1.7 \text{ ka}$ (U-Th ages) and $50.7 \pm 4.4 \text{ ka}$ ($^{39}\text{Ar}/^{40}\text{Ar}$ ages), respectively (Carrasco-Núñez et al., 2018). This effusive activity was followed by several explosive eruptions, which originated a dacitic air fall called Xoxoctic Tuff (0.6 km^3 , Ferriz and Mahood, 1984) and a pyroclastic sequence that includes an explosive breccia and pyroclastic flow deposits comprising the Llano Tuff (Ferriz and Mahood 1984; Willcox, 2011).**

The Holocene ring-fractures **fed** bimodal magmatism characterized by both explosive and effusive activity, producing several lava flows and domes, as well as **the** the ca. 7 ka (**C-14 age, Dávila-Harris and Carrasco-Núñez, 2014**) Cuicuiltic Member **during periods of dominant explosive activity. It consists of alternating pumices and scoriae erupted during contemporaneous sub-Plinian to Strombolian activity** from multiple vents located mostly along the inner **part of the caldera** and outer caldera ring faults (**Dávila-Harris and Carrasco-Núñez, 2014**). During this phase, less evolved lavas (**trachyandesite to basalt**) were erupted within and outside Los Humeros caldera, **including the olivine-bearing basaltic lava that fills the previously formed** Xalapasco crater (Fig. 1). Trachytic lava flows are the most recent activity recorded **in the area, with an age of** ca. 2.8 ka (**C-14 age, Carrasco-Núñez et al., 2017b**).

The reconstruction of the shallow stratigraphy **within** Los Potreros **caldera** is chiefly derived from **the analysis of** available **well-logs** (**Figs. 2a-b Carrasco-Núñez et al., 2017a, b**). Overall, the **post-caldera** units are lithologically dominated by lava flows resting **on** ignimbrite deposits emplaced during caldera stage. Ignimbrites of the caldera stage rest in turn on a thick sequence dominated by andesite lavas dated at ca. 1.4-2.8 Ma (**³⁹Ar/⁴⁰Ar ages, Carrasco-Núñez et al., 2017a**). The subsurface geometry of the pre- and syn-caldera products is **shown** in Figs. **2a-b, where** the in-depth geometry of the different magmatic products are cross-correlated and projected along the N-S and E-W direction, respectively. The N-S projection shows a constant depth of the top surface of the pre-caldera andesites that is associated with a highly variable depth (**down** to -400 m) of the top surface of the syn-caldera Xaltipan ignimbrite. The W-E projection shows a **higher** depth variability of both the top surface of the **pre-caldera** group (**down** to -500 m between H-19 and H-25 wells) and that of the Xaltipan ignimbrite (**down** to -400 m between H-19 and H-10 wells). Basaltic and rhyolitic-dacitic lavas **occur** at various depths (Carrasco-Núñez et al., 2017a); rhyolites-dacites are located mostly at the base (H-20 and H-26 wells) or within (H-05 well) the caldera group or the old andesite sequence (H-25 and H-19 wells). **Basalts** are located only within the pre-caldera andesite sequence, both at its base (in contact with the limestone basement; H-5 and H-8 wells) and at its top (in contact with the base of the caldera sequence; H-10 well). **These** bimodal lava products, showing an irregular lateral distribution, **have been** interpreted as subaerial (Carrasco-Núñez et al., 2017a).

The **structural architecture** of the LHVC is controlled by a network of active extensional fault systems, **made** of NNW-SSE, N-S, NE-SW and E-W **striking** fault strands cutting across the Los Potreros caldera floor. **The** following main faults were recognised (Norini et al., 2015, **2019**; Calcagno et al., 2018) (Fig.1): (i) Maxtaloya (NNW-SSE striking), (ii) Los Humeros and Loma Blanca (N-S striking), (iii) Arroyo Grande (NE-SW striking), (iv) Las Viboras and Las Papas (E-W striking). Such active fault systems **are** interpreted as due to the recent/active resurgence of the Los Potreros Caldera. **Since** the faults do not show continuity beyond the caldera border, their scarps decrease in height towards the periphery of the caldera and the dip-slip displacement vectors show a semi-radial pattern (Norini et al., 2015).

The source of the areal uplift **has been** inferred to be the inflation of a saucer or cup shaped deep magmatic source elongated NNW-SSE, **up warping** a 8 x 4 km resurgent block, centred in the SE portion of the caldera, delimited to the W by the NNW-SSE main faults, and toward the north, east and south by the caldera rim (Fig.1, Norini et al., 2015, **2019**).

The seismic activity **between** 1994-2017 is clustered along the Loma Blanca, Los Humeros and Arroyo Grande faults (Lermo et al., 2018; Fig. 1). Most of the earthquakes show a magnitude (M_w) between 1 and 2.5 and have been mainly interpreted as induced by the geothermal exploitation activity (injection of fluids and hydrofracturing; Lermo et al., 2018). **Four** major earthquakes (M_w= 3.2, 3.6, 3.9 and 4.2, at a depth of 1, 4, 2.2 and 1.8 km, respectively) have **also** been reported, with focal depths close to the trace of the active faults (Loma Blanca and Los Humeros, Fig.1). Such major earthquakes have been interpreted as triggered by fault reactivation due to fluid/brine circulation injected from geothermal wells (Lermo et al., 2018).

3 Methods

The scientific rationale adopted in this study is based on structural field work combined with analogue models aimed to constrain the depth of the deformation sources in the caldera domain. **We also tested if the relation that constrains the depth of the source deformation from surface parameters adopting elliptical sources (Brothelande and Merle 2015) is verified also for sub-circular sources.**

3.1 Structural field work

Structural field work was carried out **on the post-caldera (late Pleistocene to Holocene) deposits to characterise** the surface deformation related to the recent activity of the Los Potreros caldera **and constrain** the morphotectonic fingerprints of the resurgence **to evaluate its source and areal extent**. The geometry and distribution of the observable faults and joints were defined at the outcrop scale by measuring their attitudes (strike and dip; right-hand rule) and spacing. Fault kinematics was assessed through classical criteria on slickensides fault surfaces, such as Riedel shears, **growth fibers** and sheltering trails (Doblas, 1998). **The published geological map (Carrasco-Núñez et al., 2017b) and geothermal well data has been used (Carrasco-Núñez et al., 2017a) to correlate the surface structures at a broader scale.**

3.2 Analogue models: experimental set-up and scaling

Five experiments **were undertaken** simulating the ascent of a viscous **sub-circular** intrusion in a brittle overburden to test **the validity of** existing relationships between the depth of **elliptical intrusions** and the observed surface deformation **(Brothelande and Merle, 2015)**. The experimental set-up (Fig. 3) consists of a 31×31 cm glass box filled with a sand pack (crust analogue) of variable thickness (T , of **10**, 30 and 50 mm, respectively). In each experiment we imposed a layering using a non-cohesive marine sand below a layer of crushed silica sand (grain size = 40-200 μm , cohesion = 300 Pa), fixing the thickness ratio of the two layers (T_u/T_l) to 1, to simulate the stratigraphy in Los Potreros (stiffer post caldera lava flows above softer and less cohesive ignimbrite deposits emplaced during the caldera collapse stage). At the base of the sand pack, a piston, controlled by a **motor**, pushes upward the silicone (magma analogue) placed inside a cylinder 8 cm in diameter. The injection rate is fixed for all the experiments to 2 mm/hr and each experiment was stopped at the onset of the silicone extrusion. Both sand and silicone physical properties are listed in Table 2.

At the end of each experiment, the surface has been covered with sand to preserve their final topography and were **wetted** with water for cutting in sections to appreciate the subsurface deformation. Such sections were used to measure the mean dip of the **apical depression** faults (θ) induced by the rising silicone. A digital camera monitored the top view deformation of each experiment at 0.02 fps and a laser scanner, placed next to the camera, provided high-resolution data (maximum error ± 0.5 mm) of the vertical displacement that was used to measure in detail the geometrical features of the deformation i.e. dome diameter (L_d), **apical depression** width (L_g) and dome flank mean dip (α). According to the Buckingham-II theorem (Merle and Borgia 1996 and references therein), our models need 7 independent dimensionless numbers to be properly scaled (i.e. 10 variables minus three dimensions; Table 2). Such dimensionless numbers can be defined as the ratios (Π) listed in Table 3. **Some** values of Π_5 , **representing the ratio between the inertial and viscous forces, are very small both in** nature and experiments (1.3×10^{-20} and 6.1×10^{-10} , respectively), indicating that **the inertial forces** are **negligible with respect to the viscous forces** in both cases.

4 Results

4.1 Structural geology

The outcropping post-caldera lithologies within the Los Potreros Caldera consist of: (1) the Cuicuiltic Member, which blankets most of the surface of the upper half of the studied area; (2) basaltic lava flows filling the Xalapasco crater and the NW portion of the caldera; and (3) trachyandesitic and trachytic lava domes and thick flows extending in the southern half of the caldera and rhyolitic domes in its central part (Fig. 4). **Field work documented that** the more evolved lavas form **five nearly N-S trending** elliptical domes, **distributed in both sides of the Los Humeros Fault** (Figs. 4 and 5a): (i) a 2 km long \times 1.2 km wide trachytic dome located to the west of the Maxtaloya and Los Humeros faults, (ii) a 1×0.7 km trachyandesitic dome located **in a northeast area** of the Maxtaloya fault, and (iii) **one trachyandesitic and two obsidian smaller domes (0.4×0.2 km) to the eastern side** of the Los Humeros **Fault** (LH-11 in Fig. 4).

Field work concentrated on the three main uplifted areas corresponding to the surface expression of the Loma Blanca, Arroyo Grande and Los Humeros faults (labelled **LH1-2**, **LH9** and **LH10** respectively in Fig. 4). The observed structures in these uplifted areas (joints and faults) affect the deposits of the post-caldera phase. Based on field evidence, we also propose a revised interpretation of the surface structures identified by previous studies (Norini et al., 2015, 2019), distinguishing between lineaments (morphological linear scarps, **with no measurable fault offsets** and/or alteration at the outcrop scale), active and inactive faults, **instead** associated with **measurable fault offsets and with active or fossil alteration**, respectively (Fig. 4). We present below a description of the structures mapped in the studied area, highlighting their temporal and spatial relationships with the **post-caldera** geological formations. We identified two inactive faults (Maxtaloya and Arroyo Grande), a morphological lineament (Las Papas) and two currently active faults (Los Humeros and Loma Blanca).

4.1.1 Las Papas lineament (sites LH-07, LH-08)

The E-W trending Las Papas **lineament** is localised within the Cuicuiltic Member (LH-07; Fig. 5b). We identified an erosional surface along the scarp, where unaltered and undeformed Cuicuiltic **Member** rocks rest above **the Xoxoctic Tuff** (LH-08, Fig. 5c). The E-W trending morphological lineament **of** Las Papas **is** probably due to differential erosion of the softer layers of the pyroclastic deposits, successively blanketed by the Cuicuiltic Member.

4.1.2 Arroyo Grande (site LH-09) and Maxtaloya scarps

The NE-SW Arroyo Grande scarp (Fig. 6a) **exposes** strongly altered and faulted (NW striking faults, mean attitude $N144^\circ/68^\circ$, **number of data** (n) = 8) lavas and ignimbrites unconformably covered by the unaltered Cuicuiltic Member (Fig. 6b). The **offset** observed at the outcrop-scale for the single fault strands is **ca.** 0.5 m, with a dominant normal dip-slip kinematics (pitch angle **of the slickenlines** ranging 99° - 106°). The inferred cumulative displacement at Arroyo Grande is ~ 10 m. Similarly, an outcrop on the Maxtaloya scarp (in front of well H-6) shows altered trachyandesites covered by unaltered Cuicuiltic **Member** rocks (Fig. 6c).

4.1.3 Los Humeros (site LH-10)

The fault scarp of the N-S striking (mean attitude $N174^\circ/73^\circ$, $n = 8$) Los Humeros Fault **exposes** the altered portions of the Cuicuiltic Member. Fault population analysis reveals a dominant normal dip-slip (mean pitch angle **of the slickenlines**: 84°) kinematics, as documented by both Riedel shears and carbonate-quartz growth steps. The main fault **surface** is sutured by a trachyandesitic extrusion (Fig. 6d), localised along an aligned N-S dome (**site** LH-11 in Fig. 4).

Moreover, ~150 m southward from the outcrop of the fault scarp, a 5×3 m **wide** trachyandesitic plug shows vertical striation on its surface due to a subsurface vertical flow of the trachyandesite (Fig. 6e). The observed displacement at the outcrop scale, as indicated by the height of the fault scarp, is ~ 10 m.

4.1.4 Loma Blanca (LH-01, LH-02)

The Loma Blanca **Fault** system (**sites** LH-01 and LH-02) is located in an active degassing area, where faults and fractures are frequent. The fault system **is** on top of an elongated crest (within an **apical depression**) of a morphological bulge, ~ 1 km in **width** and 30 m in height. At this location, the Cuicuiltic Member and the underlying trachyandesite lavas are strongly altered (Fig. 6f). Evidence of stockwork veining and diffuse fracturing of the lavas suggests hydrofracturing and structurally controlled fluid flow and alteration. A set of NNE-SSW striking conjugate extensional faulting and jointing (joint spacing ~0.5 m) is observed. The faults (mean attitude $N26^{\circ}/71^{\circ}$, $n=6$) show a normal dip-slip kinematics (pitch **of the slickenlines** ranging 82° - 104°). Joint systems found in the Cuicuiltic Member strike sub-parallel to the faults (mean attitude $N37^{\circ}/72^{\circ}$, $n=14$). The inferred cumulative displacement of the faults, estimated by the depth of the **apical depression**, is ~ 5 m.

In summary, the 22 mapped faults in all the structural outcrops of the area show a main NNW-SSE strike (Fig. 6g) with a dominant dip slip movement (mean pitch angle of slickenlines 88° , $n=16$) which is sub-parallel to the N-S elongation of the lava domes and the Xalapasco crater.

4.2 Experimental results

Here we show **three representative** experiments with increasing overburden thickness (experiments **1-3-5 with T= 10, 30 and 50 mm**). Table 4 shows the measured parameters in the experiments. **Some experiments (1-2 and 3-4) were replicated with the same imposed boundary conditions and show the same result, which ensures model reproducibility.**

Overall, the experiments show a similar deformation pattern: a first stage characterized by the uplift of a sub-circular dome, bordered by inward dipping reverse faults, and a second stage characterized by the subsidence of the apical part of the dome where normal faulting occurs (**apical depression** formation Fig. 7a-i). The reverse and normal faults are ring faults and are associated with the formation of radial fractures from the dome centre. **A different shape of the apical depression is observed with $T/D > 0.12$. In exp.1 ($T/D = 0.12$) an annular peripheral depression formed as the silicone reached the surface at the edge of the cylinder (Fig.7c). Conversely, in exp. 3 and 5 ($T/D= 0.37$ and 0.63 respectively) a sub-circular apical depression formed as the silicone reached the surface at the centre of the dome (Fig.7g, m).**

Despite the T/D ratio, all the experiments show that both the dome diameter and **apical depression** width increase linearly with the overburden thickness (ranging from **105** to 164 mm and from **14** to 58 mm respectively, Table 4, Fig.8). The dome diameter increases abruptly with time, becoming almost constant at an early stage of the experiment (Fig.9a); the **apical depression** width shows a similar pattern even if it enlarges slightly with time (after the first abrupt increase) as the silicone rises towards the surface (Fig. 9b), suggesting that the intrusion depth has an higher influence on the **apical depression** width, in agreement with Brothelande and Merle (2015).

5. Discussion

5.1 Interpretation of the analogue experiments

The deformation pattern observed in the analogue experiments for thicker overburdens (experiments 3-4 and 5 with $T/D= 0.37$ and 0.63), showing a sub-circular dome and an apical depression, is in agreement with previous analogue experimental results (Acocella et al., 2001; Martí et al. 1994; Walter and Troll 2001). However, for thinner overburdens (exps. 1-2, $T/D= 0.12$), we observed a new deformation pattern at the surface consisting of an annular peripheral depression due to the rising of the silicone at the edge of the cylinder rather than its centre. We infer that in these experiments, since the rising silicone was very close to the surface, the sagging of the sand overburden pushed downward the centre of the silicone that squeezed up at the edges of the cylinder. Such process may also explain the two linear grabens that formed in the experiments with elliptical sources for small overburden thicknesses (ratio $T/D \sim 0.1$, Brothelande and Merle 2015).

The deformation pattern observed in our experiments is independent with respect to the imposed strain (i.e. uplift) rate or the viscosity of the intruding material as suggested by the similarity with results obtained in previous studies with higher strain rates (Acocella and Mulugeta, 2002) or lower viscosity intruding materials (Galetto et al., 2017; Martí et al. 1994; Walter and Troll, 2001). On the other hand, the occurrence of an apical depression is dependent on the thickness (i.e. depth) of the intrusion since thin intrusions relative to their depths will generate sub-circular domes without any apical depression (Galland et al., 2009; Galland, 2012). Moreover, our results confirm that the apical depression width shows a linear correlation with the source depth (Fig. 8) as estimated in Brothelande and Merle (2015) for elongated sources. This evidence documents that such relation is independent from the source eccentricity or shape of the extensional structures at the top of the dome (i.e. linear graben or sub-circular depression) suggesting that any elongation of the surface structure represents only a minor complication of the basic deformation pattern as already pointed out by (Roche et al., 2000).

5.2 Origin and extent of the resurgence in the LHVC

The distribution of the alteration patterns and deformation characteristics of the post caldera deposits can be used to infer the origin and extent of the uplift within the LHVC. In particular, **whether** the 7.4 ka Cuicuiltic Member **was involved** in the deformation and alteration allow **constraining** the spatio-temporal evolution of the surficial deformation and associated uplifts in Los Potreros. Unaltered and undeformed deposits of the Cuicuiltic Member crop out along the E-W Las Papas lineament and unconformably cover altered and faulted lavas and ignimbrites along the Arroyo Grande and Maxtaloya scarps. Alteration and deformation of the Cuicuiltic Member occurs along the Los Humeros Fault scarp and within the apical **depression** of the Loma Blanca bulge. **The** vertical striations of the trachyandesitic plug near the Los Humeros fault scarp suggest that the ascent of the plug induced the uplift, the normal dip-slip faulting and alteration of the Cuicuiltic **Member**.

The observations suggest that Los Potreros is not a classic resurgent caldera (i.e. a caldera characterised by a large-scale process localized in a single area) but is characterised by a discontinuous uplift process in space and time, inducing small-scale deformations at each pulse (Fig. 10a-d). In particular, it was active in the south and north-eastern sector of the caldera, at Maxtaloya and Arroyo Grande (Fig. 10a), prior to the deposition of the Cuicuiltic Member (~ 7.4 ka), and then moved towards N along the Los Humeros and Loma Blanca scarps during and post the eruption of the Cuicuiltic **Member** (Fig. 10b-d). **The** felsic lava found at the Los Humeros Fault scarp shows a similar mineral assemblage **to** the felsic domes located further south (Fig. 4); thus, the Los Humeros scarp may represent the final stage (i.e. effusive eruption of felsic magmas, (Fig. 10c) of the uplift process, which is thus driven by the ascent of relatively narrow (hundreds of meters) and highly viscous felsic magma batches. This is supported by the N-S elongation of the identified lava domes which is sub-parallel to the orientation of the measured fault planes (NNW-SSE), indicating that the observed

deformation is closely related to the post-caldera volcanism. The ascent of such magma bodies is inferred here to drive the recent uplift and deformation of the Loma Blanca bulge, as suggested by the active fumaroles and extensive alteration of both the Cuicuiltic **Member** and post-caldera lavas (Fig. 10d). The presence of such shallow magma bodies is also suggested by the four major earthquakes recorded in Los Potreros, which have been previously interpreted to be induced by geothermal exploitation (Lermo et al., 2018). However, since the magnitude of the seismic events induced by geothermal exploitation activities is usually lower (i.e. < 3, Evans et al., 2012 and references therein), the higher magnitude (between 3.2 and 4.2) of the earthquakes in Los Potreros suggests that they may be more likely of volcano-tectonic origin due to shallow magma emplacement.

To further support the above interpretation **from** field observations, **results from the presented** analogue models were used to constrain the magma source depth from the geometrical parameters measured in the experiments (L_g , θ , α , Table 4). We calculated the theoretical overburden thickness (i.e. the intrusion depth, T_t , Table 4) as follow (**Brothelande and Merle, 2015**):

$$T_t = \frac{1}{2}L_g \times \frac{\sin(\theta+\alpha)}{\cos\theta} \quad (1)$$

Comparing the percentage difference (σ) between the imposed experimental (T) and theoretical (T_t) overburden thickness values, we calculate the associated error in the evaluation of the intrusion depth in the models (σ , Table 4, Fig. 8). We then use equation (1) for the evaluation of the heat source depth at the Loma Blanca bulge considering $\sigma \sim 40\%$ (maximum value of the experiments **excluding those showing an annular depression that was not observed in the field**). For the Loma Blanca bulge $L_g = 286$ m, $\theta = 71^\circ$, $\alpha = 4.5^\circ$, the estimated intrusion depth is 425 ± 170 m. Such relatively shallow depth is within the range of depths of rhyolitic-dacitic domes drilled in geothermal wells (spanning from 300 to 1700 m, Fig. 2a-b) and is consistent with the hypothesis that the uplift is driven by small and delocalized magmatic intrusions, as suggested by the field data.

The rhyolites-dacites have been previously interpreted of subaerial origin (Carrasco-Núñez et al., 2017a), **but** we suggest that **at least some of them** can be reinterpreted as intrusions of felsic cryptodomes based on the following considerations: (i) the occurrence of rhyolite-dacite lava bodies within the thick pre-caldera old andesite sequence is unusual and does not have a subaerial counterpart; (ii) the **rhyolite body in well H-20 (Fig. 2b) up warps both the intracaldera ignimbrite sequence and the post-caldera lavas (showing a reduced thickness) indicating that the caldera forming ignimbrites do not level out the paleo-topography; and** (iii) the top of the Xaltipan ignimbrite **shows an higher** depth variation **than** the pre caldera andesite (Fig. 2a) highlighting a local and discontinuous **uplifting** of the Xaltipan ignimbrite. **Such** evidence can be more easily reconciled with the intrusion of felsic cryptodomes within the volcanic sequence, **rather than with** a regular layer-cake stratigraphy.

5.3 Implications for the structure of the LHVC geothermal field

The combination of field and modelling data support that the uplift in Los Potreros **caldera** is due to multiple deformation sources in narrow areas that do not represent resurgence *sensu stricto*. Such localized recent deformation within Los Potreros caldera appears to be linked to small magmatic intrusions located at relatively shallow depths (i.e. < 1 km) as in Loma Blanca, where the estimated intrusion depth calculated from the experimental data is 425 ± 170 m.

This model **differs** from the general accepted idea of resurgence in Los Potreros induced by the inflation of a saucer or cup shaped deep magmatic intrusion (Norini et al., 2015, 2019). The resurgence is inferred to be centred beneath the sector of the caldera traversed by the E-W lineaments and limited by the Maxtaloya and Arroyo Grande faults (sector S1 in Norini et al., 2015). The thermal anomalies identified by Norini et al. (2015) show that the temperatures are unexpectedly cold beneath the inferred centre of the resurgent block, where the highest temperatures should be expected.

By contrast, sharp and narrow temperature peaks, spatially coincident with Los Humeros and Loma Blanca faults, are consistent with the presence of shallow and delocalized heat sources. Indeed, the inflation of the deep magma chamber of the LHVC, inferred to be at 5 to 7-8 km of depth (Verma, 1983, 2000, 2011) and extending 9 km in radius and 6 km in length (thus coinciding with the Los Humeros caldera rim, Verma et al., 1990), should have resulted in a much wider uplift and with higher magnitude than the one observed in the field. Resurgence resulting from magma remobilization of the deep chamber that produced collapse is characterized by a larger-scale surface deformation (thousands of meters of uplift extending for tens of kilometers on the surface) as shown in many large calderas worldwide (Toba, de Silva et al., 2015; Cerro Galan, Folkes et al., 2011; Ischia, Carlino, 2012).

It is therefore unlikely that the replenishment of new magma in the caldera forming deep magma chamber accounts for the magnitude (few tens of meters) and discontinuous spatial distribution of the deformation in Los Potreros.

Such a model of the recent uplifting in Los Potreros is supported by field-based petrographic-mineralogical analysis showing that the present-day magmatic plumbing system is characterized by multiple magma levels spanning from a deep (30-33 km) basaltic reservoir to very shallow (~ 1.5 km), smaller, trachyandesitic-trachytic magma batches (Lucci et al., under review).

A similar model of the plumbing system has been proposed to explain the eruptive activity of Usu volcano (Japan) since 1663, a post caldera cone of the Toya caldera consisting of a basaltic main edifice surmounted by 3 felsic lava domes and more than 10 cryptodomes. Petrochemical data at Usu suggest the presence of multiple magma batches (i.e. sills) at 0.25-2 km deep that originated from partial melting of a metagabbro (Matsumoto and Nakagawa, 2010; Tomya et al., 2010). Our proposed model has implications for planning future geothermal exploration: siting of future geothermal wells should consider that the presence of shallow heat sources within the caldera may complicate the pattern of isotherms associated with the deeper heat flow.

6 Conclusions

By integrating field work with analogue models, we constrain the late Pleistocene-Holocene spatio-temporal evolution of volcanism of the LHVC and estimate the depth of the magmatic intrusions feeding the active geothermal system. New findings on experimental analogue models of resurgent domes are also provided.

These are the main results that can be extracted from this study:

1. The distribution of the alteration patterns and deformation of the Cuicuiltic Member suggests that the recent (post-caldera collapse) uplift in Los Potreros caldera moved progressively northwards, from the south and north-eastern sector of the caldera towards N along the Los Humeros and Loma Blanca scarps.
2. The estimated depth of the intrusions responsible for such uplift is very shallow, as calculated from the experimental data for the Loma Blanca bulge (425 ± 170 m).
3. The recent uplift in Los Potreros is discontinuous in space and time, inducing small-scale (areal extent ~ 1 km²) deformations originating from multiple and shallow (< 1 km depth) magmatic bodies, thus not representing a classic resurgent caldera, which usually involves large scale deformation (areal extent of several km²).
4. The relation that relates the magmatic source depth with the surface parameters of resurgent domes is independent by the source eccentricity, similarly to what already verified for sub-circular intrusions.

Acknowledgements

CFE is kindly acknowledged for allowing work on the Los Humeros geothermal field. Federico Galetto helped for laser scanner data processing. Fabio Corbi and Matteo Trolese provided technical support in building the experimental set-up.

Gianluca Norini is acknowledged for logistic support in the field. Alessandra Pensa kindly helped with figure drawings. Funded by the European Union's Horizon 2020 GEMex Project (grant agreement No. 727550) and by the Mexican Energy Sustainability Fund CONACYT-SENER, WP 4.5 of the Project 2015-04-268074. More information can be found on the GEMex Website: <http://www.gemex-h2020.eu>. The Grant to Department of Science, Roma Tre University (MIUR-Italy Dipartimenti di Eccellenza, ARTICOLO 1, COMMI 314 – 337 LEGGE 232/2016) is gratefully acknowledged.

References

Acocella, V.: Great challenges in volcanology: how does the volcano factory work?, *Front. Earth Sci.*, 2:4, <https://doi.org/10.3389/feart.2014.00004>, 2014.

Acocella, V., and Funicello, R.: The interaction between regional and local tectonics during resurgent doming: the case of the island of Ischia, Italy, *J. Volcanol. Geoth. Res.*, 88, 109-123, [https://doi.org/10.1016/S0377-0273\(98\)00109-7](https://doi.org/10.1016/S0377-0273(98)00109-7), 1999.

Acocella, V., and Mulugeta, G.: Experiments simulating surface deformation induced by pluton emplacement, *Tectonophysics*, 352, 275-293, [https://doi.org/10.1016/S0040-1951\(02\)00218-4](https://doi.org/10.1016/S0040-1951(02)00218-4), 2002.

Acocella, V., Cifelli, F., and Funicello, R.: The control of overburden thickness on resurgent domes, *J. Volcanol. Geoth. Res.*, 111, 137–153, [https://doi.org/10.1016/S0377-0273\(01\)00224-4](https://doi.org/10.1016/S0377-0273(01)00224-4), 2001.

Arellano, V.M., García, A., Barragán, R.M., Izquierdo, G., Aragón, A., and Nieva, D.: An updated conceptual model of the Los Humeros geothermal reservoir (Mexico), *J. Volcanol. Geoth. Res.*, 124, 67–88, [https://doi.org/10.1016/S0377-0273\(03\)00045-3](https://doi.org/10.1016/S0377-0273(03)00045-3), 2003.

Beavon, R.V.: A resurgent cauldron in the early Paleozoic of Wales, U.K., *J. Volcanol. Geoth. Res.*, 7, 157-174, [https://doi.org/10.1016/0377-0273\(80\)90025-6](https://doi.org/10.1016/0377-0273(80)90025-6), 1980.

Brothelande, E., Peltier, A., Got, J.L., Merle, O., Lardy, M., and Garaebiti, E.: Constraints on the source of resurgent doming inferred from analogue and numerical modeling — Implications on the current feeding system of the Yenkahe dome–Yasur volcano complex (Vanuatu), *J. Volcanol. Geoth. Res.*, 322, 225–240, <https://doi.org/10.1016/j.jvolgeores.2015.11.023>, 2016.

Brothelande, E., and Merle, O.: Estimation of magma depth for resurgent domes: An experimental approach, *Earth Planet. Sc. Lett.*, 412, 143–151, <https://doi.org/10.1016/j.epsl.2014.12.011>, 2015.

Calcagno, P., Evanno, G., Trumpy, E., Carlos Gutiérrez-Negrín, L., Macías, J.L., Carrasco-Núñez, G., and Liotta, D.: Preliminary 3-D geological models of Los Humeros and Aocolulco geothermal fields (Mexico)-H2020 GEMex Project, *Adv. Geosci.*, 45, 321–333, <https://doi.org/10.5194/adgeo-45-321-2018>, 2018.

Carlino, S.: The process of resurgence for Ischia Island (southern Italy) since 55 ka: The laccolith model and implications for eruption forecasting, *B. Volcanol.*, 74, 947–961. <https://doi.org/10.1007/s00445-012-0578-0>, 2012.

Carrasco-Núñez, G., and Branney, M.J.: Progressive assembly of a massive layer of ignimbrite with a normal-to-reverse compositional zoning: The Zaragoza ignimbrite of central Mexico, *B. Volcanol.*, 68, 3–20, <https://doi.org/10.1007/s00445-005-0416-8>, 2005.

Carrasco-Núñez, G., McCurry, M., Branney, M.J., Norry, M., and Willcox, C.: Complex magma mixing, mingling, and withdrawal associated with an intra-Plinian ignimbrite eruption at a large silicic caldera volcano: Los Humeros of central Mexico, *Bull. Geol. Soc. Am.*, 124, 1793–1809, <https://doi.org/10.1130/B30501.1>, 2012.

Carrasco-Núñez, G., López-Martínez, M., Hernández, J., and Vargas, V.: Subsurface stratigraphy and its correlation with the surficial geology at Los Humeros geothermal field, eastern Trans-Mexican Volcanic Belt, *Geothermics*, 67, 1–17, <https://doi.org/10.1016/j.geothermics.2017.01.001>, 2017a.

Carrasco-Núñez, G., Hernández, J., De León, L., Dávila, P., Norini, G., Bernal, J.P., Jicha, B., Navarro, M., López-Quiroz, P., and Digitalis, T.: Geologic Map of Los Humeros volcanic complex and geothermal field, eastern Trans-Mexican Volcanic Belt, *Terra Digitalis*, 1, 1–11, <https://doi.org/10.22201/igg.terradigitalis.2017.2.24.78>, 2017b.

Carrasco-Núñez, G., Bernal, J.P., Dávila, P., Jicha, B., Giordano, G., and Hernández, J.: Reappraisal of Los Humeros volcanic complex by new U/Th zircon and ⁴⁰Ar/³⁹Ar dating: Implications for greater geothermal potential, *Geochem. Geophys. Geosy.*, 19, 132-149, <https://doi.org/10.1002/2017GC007044>, 2018.

Catalano, S., De Guidi, G., Lanzafame, G., Monaco, C., and Tortotici, L.: Late quaternary deformation on the island on Pantelleria: new constraints for the recent tectonic evolution of the Sicily Channel Rift (southern Italy). *J. Geodyn.* 48, 75–82, 2009.

Chang, W.L., Smith, R.B., Wicks, C., Farrell, J.M., and Puskas, C.M.: Accelerated uplift and magmatic intrusion of the Yellowstone Caldera, 2004 to 2006, *Science*, 318, 952-956, <https://doi.org/10.1126/science.1146842>, 2007.

Christiansen, R.L., Lipman, P.W., Carr, W.J., Byers, F.M., Orkild, P.P., and Sargent, K.A.: Timber Mountain-Oasis Valley caldera complex of southern Nevada, *Geol. Soc. Am. Bull.*, 88, 943-959, [https://doi.org/10.1130/0016-7606\(1977\)88<943:TMVCCO>2.0.CO;2](https://doi.org/10.1130/0016-7606(1977)88<943:TMVCCO>2.0.CO;2), 1977.

Dávila-Harris, P., and Carrasco-Núñez, G.: An unusual syn-eruptive bimodal eruption: The Holocene Cuicuiltic Member at Los Humeros caldera, Mexico, *J. Volcanol. Geoth. Res.*, 271, 24–42, <https://doi.org/10.1016/j.jvolgeores.2013.11.020>, 2014.

de Silva, S.L., Mucek, A.E., Gregg, P.M., and Pratomo, I.: Resurgent Toba - field, chronologic, and model constraints on time scales and mechanisms of resurgence at large calderas, *Front. Earth Sci.*, 3, 1–17, <https://doi.org/10.3389/feart.2015.00025>, 2015.

Doblas, M.: Slickenside kinematic indicators, *Tectonophysics*, 295, 187–197, [https://doi.org/10.1016/S0040-1951\(98\)00120-6](https://doi.org/10.1016/S0040-1951(98)00120-6), 1998.

Du Bray, E.A., and Pallister, J.S.: Recrystallization and anatexis along the plutonic–volcanic contact of the Turkey Creek caldera, Arizona, *Geol. Soc. Am. Bull.*, 111, 143–153, [https://doi.org/10.1130/0016-7606\(1999\)111<0143:RAAATP>2.3.CO;2](https://doi.org/10.1130/0016-7606(1999)111<0143:RAAATP>2.3.CO;2), 1999.

Elston, W.: Mid-Tertiary ash flow tuff cauldrons, southwestern New Mexico, *J. Geophys. Res.*, 89, 8733–8750, <https://doi.org/10.1029/JB089iB10p08733>, 1984.

Evans, K.F., Zappone, A., Kraft, T., Deichmann, N., and Moia, F.: A survey of the induced seismic responses to fluid injection in geothermal and CO₂ reservoirs in Europe, *Geothermics*, 41, 30-54, <https://doi.org/10.1016/j.geothermics.2011.08.002>, 2012.

Ferrari, L., Orozco-Esquivel, T., Manea, V., and Manea, M.: The dynamic history of the Trans-Mexican Volcanic Belt and the Mexico subduction zone, *Tectonophysics*, 522–523, 122–149, <https://doi.org/10.1016/j.tecto.2011.09.018>, 2012.

Ferriz, H., and Mahood, G.A.: Eruption Rates and Compositional Trends at Los Humeros Volcanic Center, Puebla, Mexico, *J. Geophys. Res.*, 89, 8511-8524, <https://doi.org/10.1029/JB089iB10p08511>, 1984.

Folkes, C.B., Wright, H.M., R.A.F. Cas, de Silva, S.L., Lesti, C., and Viramonte, J.G.: A re-appraisal of the stratigraphy and volcanology of the Cerro Galán volcanic system, NW Argentina, *B. Volcanol.*, 73, 1427–1454, <https://doi.org/10.1007/s00445-011-0459-y>, 2011.

Fridrich, C.J., Smith, R.P., DeWitt, E., McKee, E.H.: Structural, eruptive, and intrusive evolution of the Grizzly Peak caldera, Sawatch Range, Colorado, *Geol. Soc. Am. Bull.*, 103, 1160-1177, [https://doi.org/10.1130/0016-7606\(1991\)103<1160:SEAIEO>2.3.CO;2](https://doi.org/10.1130/0016-7606(1991)103<1160:SEAIEO>2.3.CO;2), 1991.

- Galetto, F., Acocella, V., and Caricchi, L.: Caldera resurgence driven by magma viscosity contrasts, *Nat. Commun.*, 8, 1–11, <https://doi.org/10.1038/s41467-017-01632-y>, 2017.
- Galetto, F., Bagnardi, M., Acocella, V., and Hooper, A.: Noneruptive unrest at the caldera of Alcedo Volcano (Galápagos Islands) revealed by InSAR data and geodetic modelling, *J. Geophys. Res.*, 124, 3365–3381, <https://doi.org/10.1029/2018JB017103>, 2019.**
- Galland, O.: Experimental modelling of ground deformation associated with shallow magma intrusions, *Earth Planet. Sc. Lett.*, 317-318, 145-156, <https://doi.org/10.1016/j.epsl.2011.10.017>, 2012.**
- Galland, O., Planke, S., Ragnhild Neumann, E., and Malthe-Sørensen, A.: Experimental modelling of shallow magma emplacement: Application to saucer-shaped intrusions, *Earth Planet. Sc. Lett.*, 277, 373-383, <https://doi.org/10.1016/j.epsl.2008.11.003>, 2009.**
- Goto, Y., and McPhie, J.: Tectonics, structure, and resurgence of the largest Quaternary caldera in Japan: Kutcharo, Hokkaido, *Geol. Soc. Am. Bull.*, 130, 1307-1322, <https://doi.org/10.1130/B31900.1>, 2018.**
- Guillou-Frottier, L., Burov, E.B., and Milési, J.P.: Genetic links between ash-flow calderas and associated ore deposits as revealed by large-scale thermo-mechanical modelling, *J. Volcanol. Geoth. Res.*, 102, 339–361, [https://doi.org/10.1016/S0377-0273\(00\)00246-8](https://doi.org/10.1016/S0377-0273(00)00246-8), 2000.
- Hildreth, W., Fierstein, J., and Calvert, A.: Early postcaldera rhyolite and structural resurgence at Long Valley Caldera, California, *J. Volcanol. Geoth. Res.*, 335, 1-34, <http://dx.doi.org/10.1016/j.jvolgeores.2017.01.005>, 2017.**
- Kennedy, B., Wilcock, J., and Stix, J.: Caldera resurgence during magma replenishment and rejuvenation at Valles and Lake City calderas, *B. Volcanol.*, 74, 1833–1847, <https://doi.org/10.1007/s00445-012-0641-x>, 2012.
- Lipman, P. W.: The roots of ash flow calderas in Western North America: windows into the tops of granitic batholiths, *J. Geophys. Res.*, 89, 8801–8841, <https://doi.org/10.1029/JB089iB10p08801>, 1984.**
- Lermo, J., Lorenzo, C., Jiménez, N., Ramos, E., Ângulo, J., Israel, J., Téllez, N., Machado, O., Álvarez, I., Torres, R., Alfaro R.: Analisis de la actividad sísmica (1994-2016), su relación con los pozos inyectoros y productores y aplicación de nuevas técnicas geofísica para caracterizar las zonas anómalas del campo geotérmico de Los Humeros, CEMIE-GEO, Mexico, Internal Rep., 42 pp., 2018.
- Lucci, F., Carrasco-Núñez, G., Rossetti, F., Theye, T., White, J. C., Urbani, S., Azizi, H., Asahara, Y., and Giordano, G.: Anatomy of the magmatic plumbing system of Los Humeros Caldera (Mexico): implications for geothermal systems, *Solid Earth Discuss.*, <https://doi.org/10.5194/se-2019-86>, in review, 2019.
- Marsh, B.D.: On the mechanics of caldera resurgence, *J. Geophys. Res.*, 89, 8245–8251, <https://doi.org/10.1029/JB089iB10p08245>, 1984.
- Marti, J., Ablay, G.J., Redshaw, L.T., and Sparks, R.S.J.: Experimental studies of collapse calderas, *J. Geol. Soc. London*, 151, 919-929, <https://doi.org/10.1144/gsjgs.151.6.0919>, 1994.**
- Merle, O., Borgia, A.: Scaled experiments of volcanic spreading, *J. Geophys. Res.*, 101, 13805-13817, <https://doi.org/10.1029/95JB03736>, 1996.
- Morán-Zenteno, D.J., Alba-Aldave, L.A., Solé, J., and Iriondo, A.: A major resurgent caldera in southern Mexico: the source of the late Eocene Tizapotala ignimbrite. *J. Volcanol. Geoth. Res.*, 136, 97–119, <https://doi.org/10.1016/j.jvolgeores.2004.04.002>, 2004.**
- Moretti, R., Troise, C., Sarno, F., and De Natale, G.: Caldera unrest driven by CO₂ induced drying of the deep hydrothermal system, *Sci. Rep. UK*, 8, <https://doi.org/10.1038/s41598-018-26610-2>, 2018.**
- Mueller, W.U., Stix, J., Corcoran, P.L., Daigneault, R.: Subaqueous calderas in the Archean Abitibi greenstone belt: An overview and new ideas, *Ore Geol. Rev.*, 35, 4–46, <https://doi.org/10.1016/j.oregeorev.2008.12.003>, 2009.

Norini, G., Groppelli, G., Sulpizio, R., Carrasco-Núñez, G., Dávila-Harris, P., Pelliccioli, C., Zucca, F., and De Franco, R.: Structural analysis and thermal remote sensing of the Los Humeros Volcanic Complex: Implications for volcano structure and geothermal exploration, *J. Volcanol. Geoth. Res.*, 301, 221–237, <https://doi.org/10.1016/j.jvolgeores.2015.05.014>, 2015.

Norini, G., Carrasco-Núñez, G., Corbo-Camargo, F., Lermo, J., Hernández Rojas, J., Castro, C., Bonini, M., Montanari, D., Corti, G., Moratti, G., Chavez, G., Ramirez, M., and Cedillo F.: The structural architecture of the Los Humeros volcanic complex and geothermal field, *J. Volcanol. Geoth. Res.*, 381, 312-329. <https://doi.org/10.1016/j.jvolgeores.2019.06.010>, 2019.

Matsumoto, A., and Nakagawa, M.: Formation and evolution of silicic magma plumbing system: Petrology of the volcanic rocks of Usu volcano, Hokkaido, Japan, *J. Volcanol. Geoth. Res.*, 196, 185–207, <https://doi.org/10.1016/j.jvolgeores.2010.07.014>, 2010.

Pribnow, D.F.C., Schütze, C., Hurter, S.J., Flechsig, C., Sass, J.H.: Fluid flow in the resurgent dome of Long Valley Caldera: Implications from thermal data and deep electrical sounding. *J. Volcanol. Geoth. Res.*, 127, 329–345, [https://doi.org/10.1016/S0377-0273\(03\)00175-6](https://doi.org/10.1016/S0377-0273(03)00175-6), 2003.

Roche, O., Druitt, T.H., and Merle, O.: Experimental study of caldera formation, *J. Geophys. Res.*, 105, <https://doi.org/10.1029/1999JB900298>, 395-416, 2000.

Smith, R. L., and Bailey, R. A.: Resurgent cauldrons, *Geol. Soc. Am. Mem.*, 116, 613–662, <https://doi.org/10.1130/MEM116>, 1968.

Stix, J., Kennedy, B., Hannington, M., Gibson, H., Fiske, R., Mueller, W., Franklin, J.: Caldera-forming processes and the origin of submarine volcanogenic massive sulfide deposits, *Geology*, 31, 375–378, [https://doi.org/10.1130/0091-7613\(2003\)031<0375:CFPATO>2.0.CO;2](https://doi.org/10.1130/0091-7613(2003)031<0375:CFPATO>2.0.CO;2), 2003.

Swanson, E., and McDowell, F.: Geology and geochronology of the Tomochic caldera, Chihuahua, Mexico, *Geol. Soc. Am. Bull.*, 96, 1477-1482, [https://doi.org/10.1130/0016-7606\(1985\)96<1477:GAGOTT>2.0.CO;2](https://doi.org/10.1130/0016-7606(1985)96<1477:GAGOTT>2.0.CO;2), 1985.

Tomiya, A., Takahashi, E., Furukawa, N., Suzuki, T.: Depth and evolution of a silicic magma chamber: Melting experiments on a low-K rhyolite from Usu volcano, Japan, *J. Petrol.*, 51, 1333–1354, <https://doi.org/10.1093/petrology/egg021>, 2010.

Ueda, H., Nagai, M., and Tanada, T.: Phreatic eruptions and deformation of Ioto Island (Iwo-jima), Japan, triggered by deep magma injection, *Earth Planets Space*, 70, <https://doi.org/10.1186/s40623-018-0811-y>, 2018.

Verma, M.P., Verma, S.P., and Sanvicente, H.: Temperature field simulation with stratification model of magma chamber under Los Humeros caldera, Puebla, Mexico, *Geothermics*, 19, 187–197, [https://doi.org/10.1016/0375-6505\(90\)90015-4](https://doi.org/10.1016/0375-6505(90)90015-4), 1990.

Verma, S.P., Gómez-Arias, E., and Andaverde, J.: Thermal sensitivity analysis of emplacement of the magma chamber in Los Humeros caldera, Puebla, Mexico, *Int. Geol. Rev.*, 53, 905–925, <https://doi.org/10.1080/00206810903234296>, 2011.

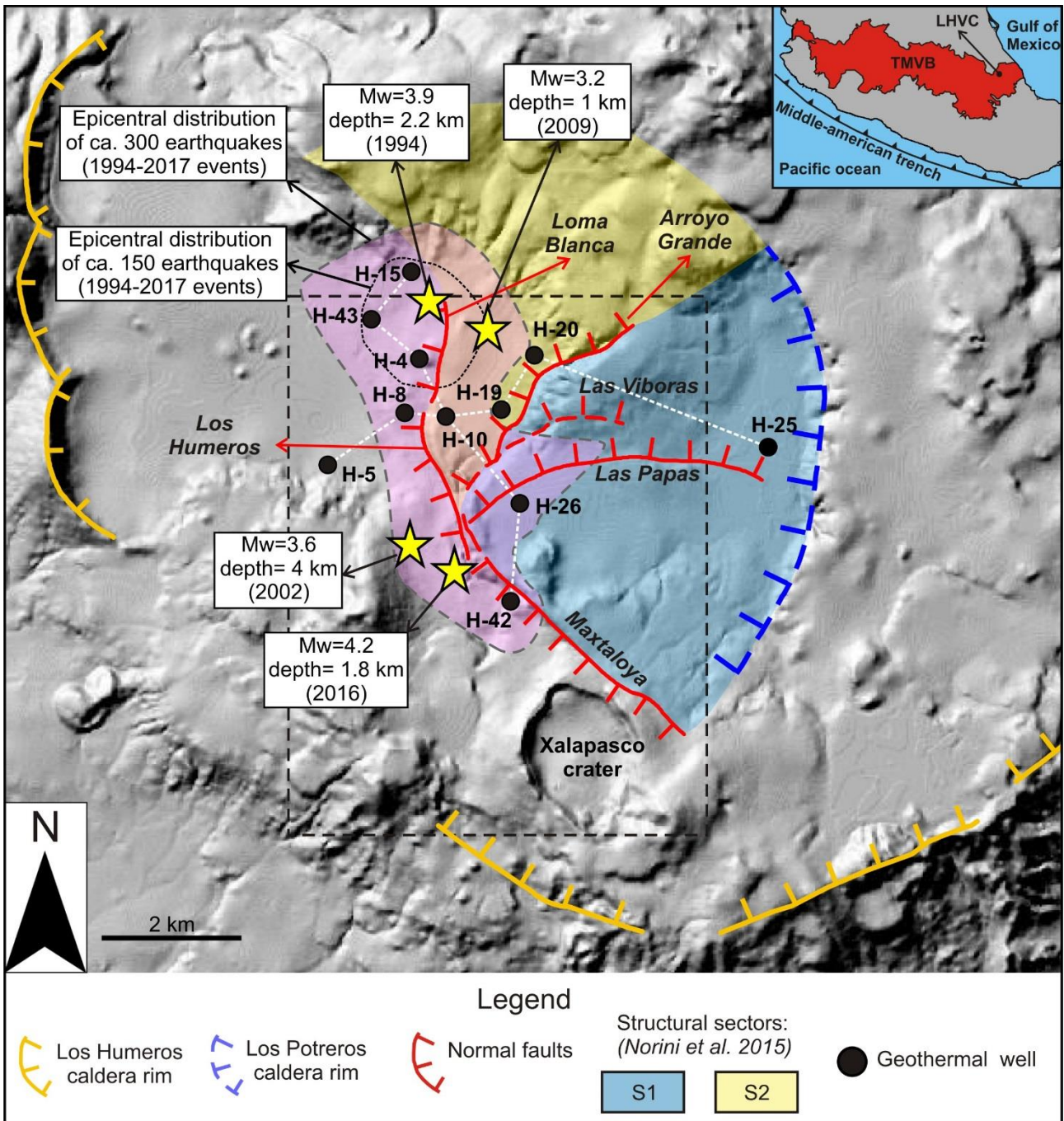
Verma, S.P.: Magma genesis and chamber processes at Los Humeros caldera, Mexico - Nd and Sr isotope data, *Nature*, 302, 52–55, <https://doi.org/10.1038/302052a0>, 1983.

Verma, S.P.: Geochemical evidence for a lithospheric source for magmas from Los Humeros caldera, Puebla, Mexico. *Chem. Geol.* 164, 35–60, [https://doi.org/10.1016/S0009-2541\(99\)00138-2](https://doi.org/10.1016/S0009-2541(99)00138-2), 2000.

Walter, T.R., and Troll, V.R.: Formation of caldera periphery faults: an experimental study, *B. Volcanol.*, 63, 191-203, <https://doi.org/10.1007/s004450100135>, 2001.

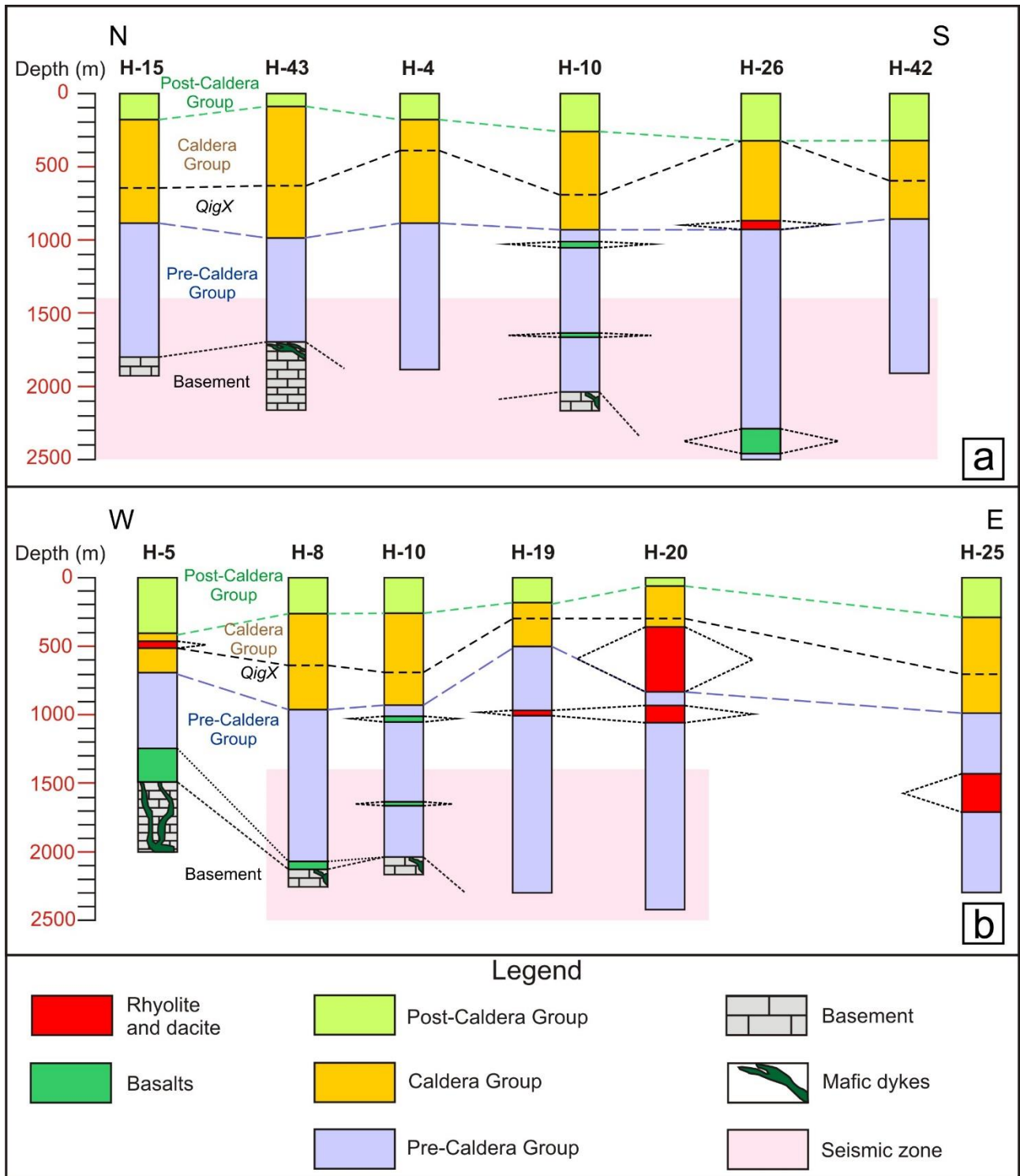
Walter, T.R., Wang, R., Acocella, V., Neri, M., Grosser, H., and Zschau, J: Simultaneous magma and gas eruptions at three volcanoes in southern Italy: an earthquake trigger ?, *Geology*, 37, 251–254, <https://doi.org/10.1130/G25396A>, 2009.

Wilcox, C.P.: Eruptive, magmatic and structural evolution of a large explosive caldera volcano, Los Humeros, Central Mexico, Ph.D. thesis, Department of Geology, University of Leicester, United Kingdom, 317 pp., 2011.



1
 2 **Figure 1:** Shaded relief image (illuminated from the NE) obtained from 15 m resolution DEM of the Los Humeros Volcanic
 3 Complex (LHVC) showing the main structural features (faults and caldera rim, modified from Norini et al. (2015); Calcagno
 4 et al. (2018) and some geothermal wells referred in the text and in Figures 2a-b. The white dashed lines indicate the direction
 5 of the correlation sections shown in Figures 2a-b. The black rectangle indicates the studied area within the Los Potreros Caldera
 6 shown in Figure 4. The Inset box show the location of the LHVC (black dot and arrow) within the eastern sector of the Trans
 7 Mexican Volcanic Belt (TMVB). The structural sectors S1 and S2 correspond to the resurgent block inferred by Norini et al.
 8 (2015). Seismicity data from Lermo et al. (2018).

9
 10
 11
 12
 13



14
 15 **Figure 2: In depth correlation of lithostratigraphic units along the N-S (a) and W-E (b) direction (redrawn after Carrasco-**
 16 **Núñez et al. (2017a) and Arellano et al. (2003). Depth:horizontal distance=1:1. Location of the correlation line is shown in**
 17 **Figure 1. QigX= Xaltipan ignimbrite.**

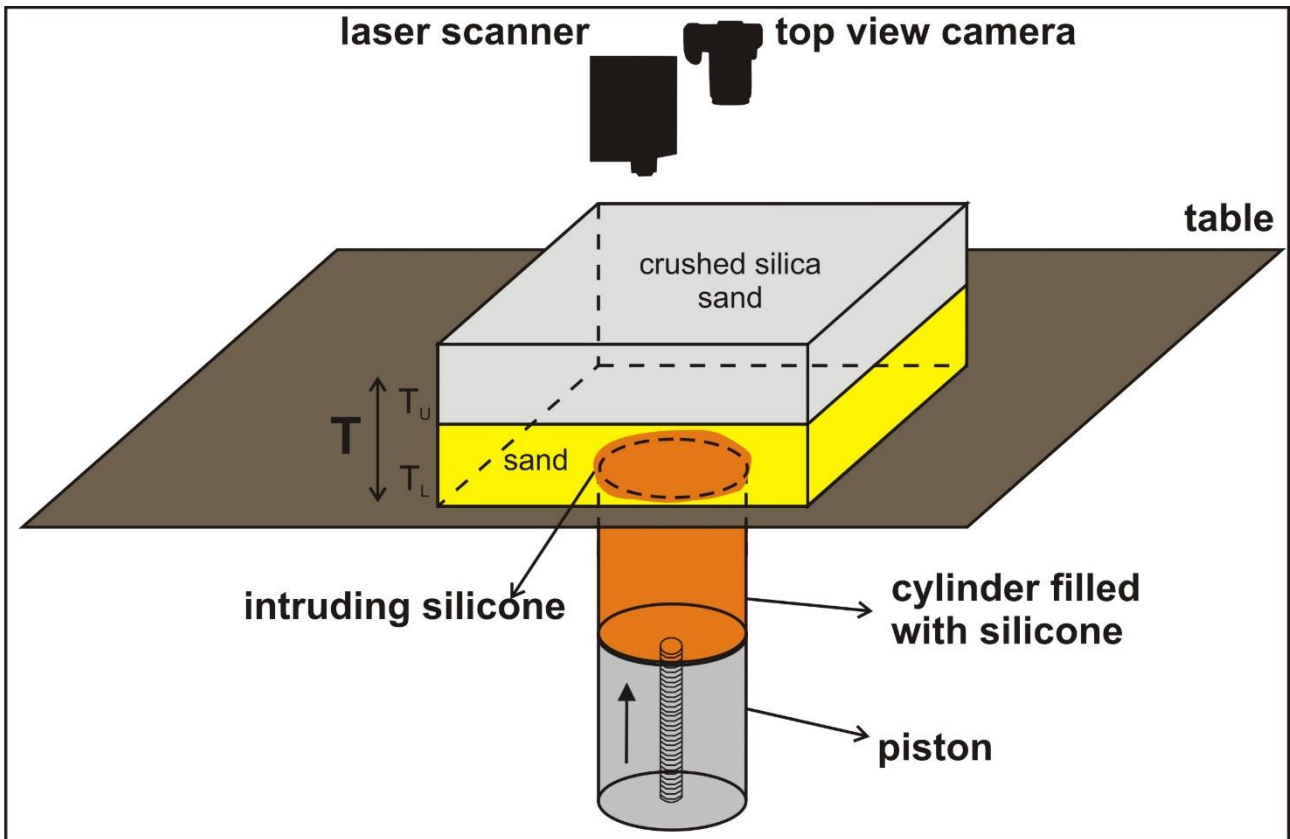


Figure 3: Experimental set-up. A motor controlled piston pushes upward the silicone at a fixed rate (2mm/hr) from the base of the layered sand pack (the diameter of the silicone is 8 cm). A laser scanner and a camera record the surface deformation induced by the intruding silicone. T = total overburden thickness, T_U = upper layer thickness, T_L = lower layer thickness.

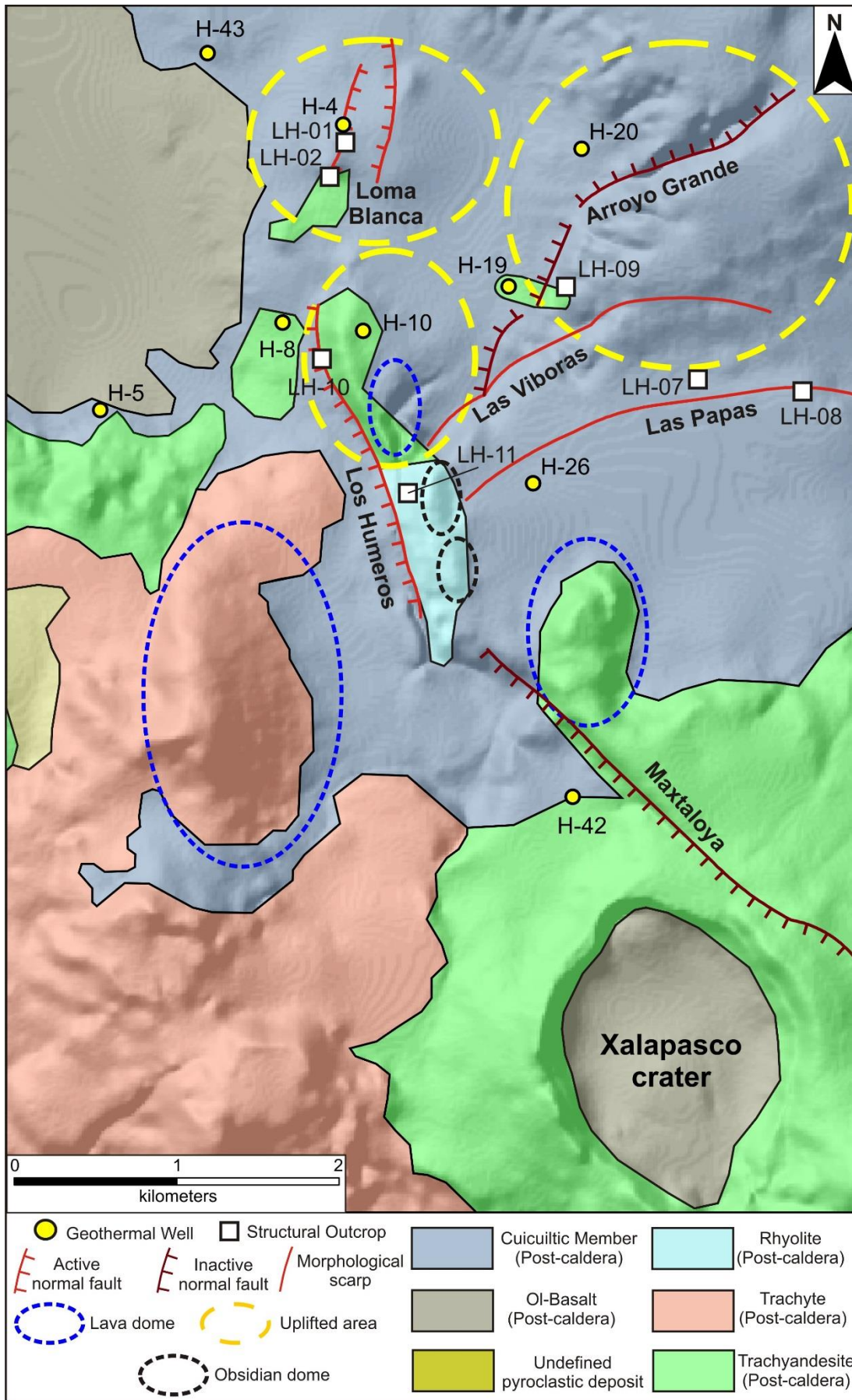


Figure 4: Simplified geological structural map of the studied area; reinterpreted after (Norini et al., 2015; Carrasco- Núñez et al., 2017b; Calcagno et al., 2018).



Figure 5: a) Panoramic view from Xalapasco crater (looking towards N) of the lava domes aligned N-S. b) Unaltered Cuicuiltic Member (LH-07). c) Unaltered Cuicuiltic Member covering a layered pyroclastic deposit, which can be laterally correlated with the Xoxoctic Tuff (LH-08). The erosional surface preceding the deposition of the Cuicuiltic Member is shown (dashed white line).

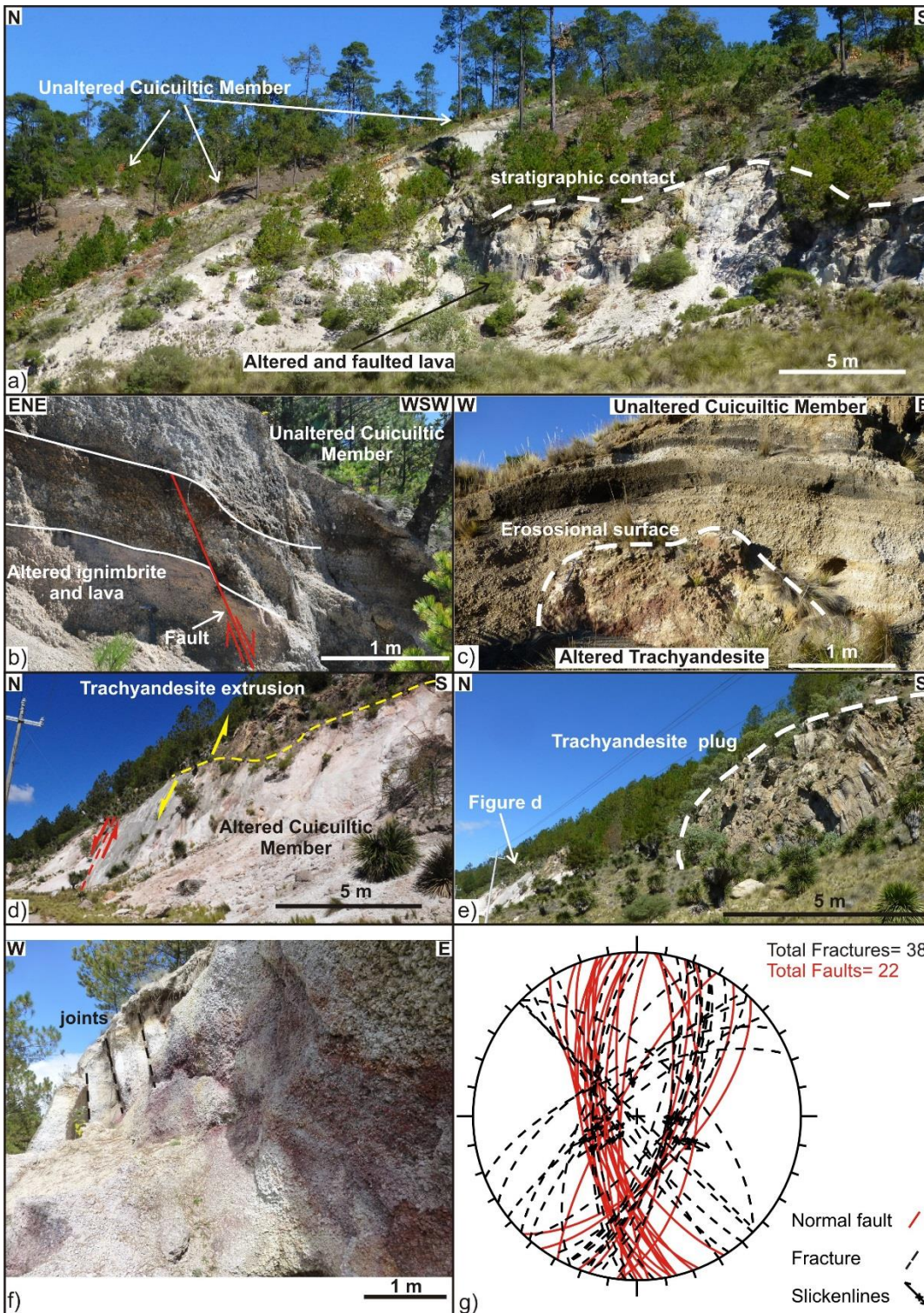


Figure 6: a) Panoramic view of the Arroyo Grande fault scarp showing the unaltered Cuicuiltic Member covering the altered and faulted ignimbrite and lavas (site LH-09). b) Normal fault affecting the altered ignimbrite deposits unconformably covered by the post-caldera, unaltered Cuicuiltic Member deposits (LH-09). Note that the Cuicuiltic Member deposits are not faulted at this location; the fault can be thus considered as a fossil fault with respect to the Cuicuiltic Member deposition. c) Block of altered trachyandesite buried by unaltered Cuicuiltic Member layers along the Maxtaloya fault scarp. d) Los Humeros fault scarp (LH-10) induced by the ascent of the trachyandesitic extrusion on top of the fault plane. e) Trachyandesite plug cropping out ~150 southward the fault scarp shown in d) (indicated by the red arrow). f) Jointing and alteration of the Cuicuiltic Member within the apical depression of the Loma Blanca dome (LH-01). g) Equal-area stereo-plot of the attitudes of faults and fractures in all the structural outcrops.

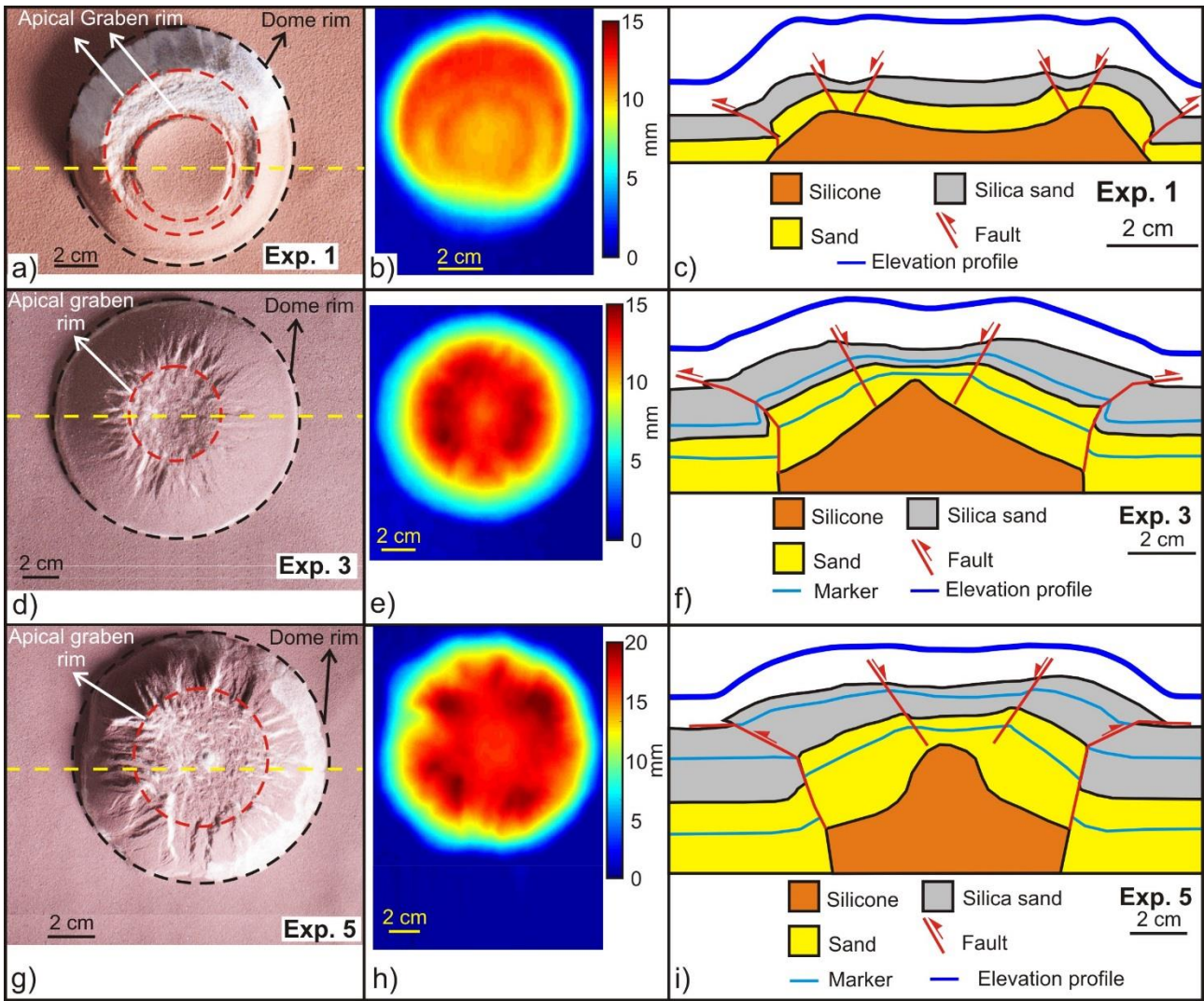


Figure 7: a) d) g) Top view image of the experiments 1, 3 and 5. b) e) h) cumulative vertical displacement; colour scale is proportional to the amount of uplift. c) f) i) Drawing of the cross section view obtained after cutting the section close to the dome center. The elevation profiles are obtained from laser scanner data. The yellow dashed line in a) d) g) indicates the trace of the section views and of the elevation profiles.

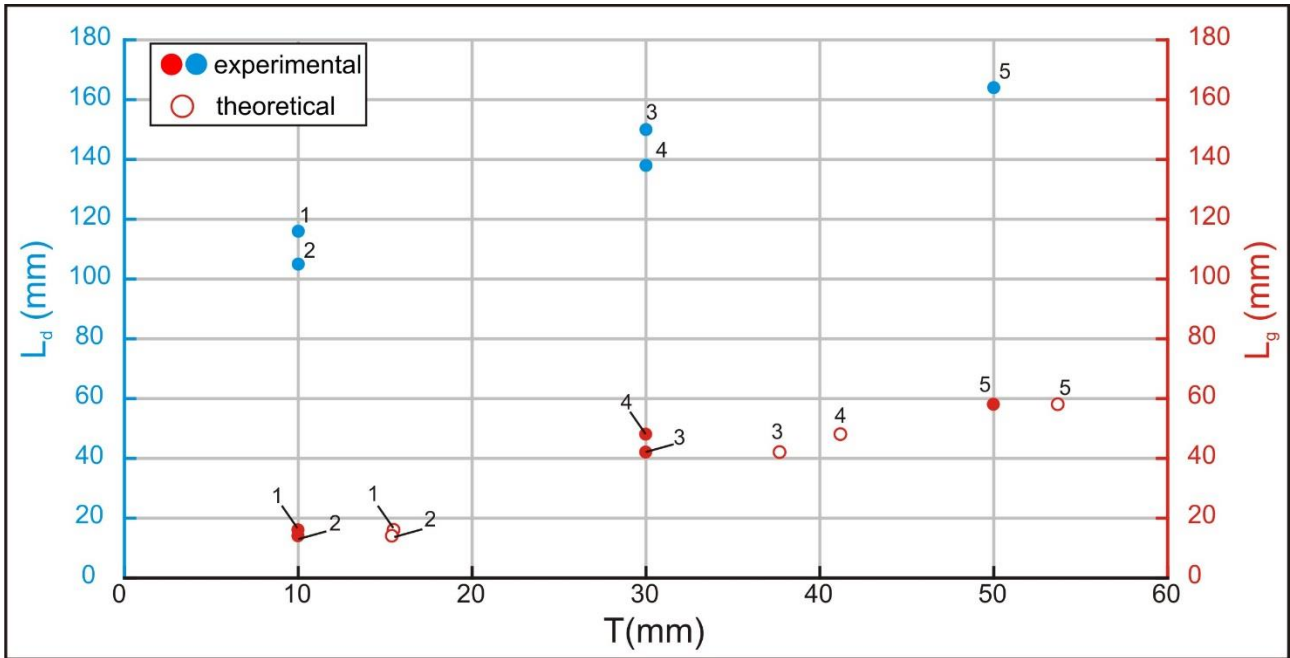


Figure 8: L_g (apical depression width) and L_d (dome diameter) versus T (overburden thickness). Theoretical values calculated after equation 1 (see discussion section). The numbers above each point indicate the experiment number.

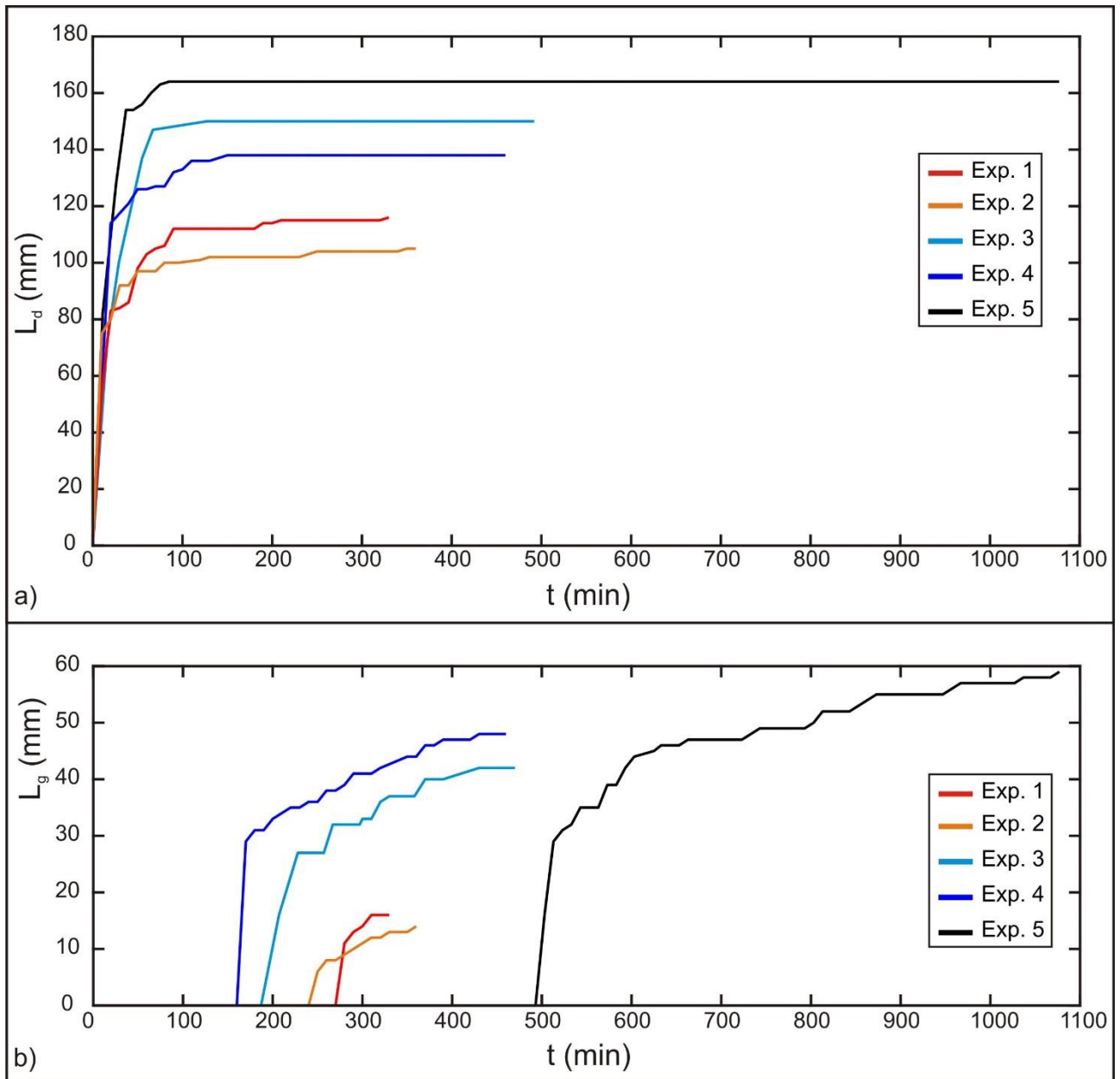


Figure 9: a) Time evolution of the dome diameter (L_d). b) Time evolution of the apical depression width (L_g). Both L_d and L_g show a similar evolution trend with a first stage of abrupt increase at the beginning of each experiment. In the second stage L_d becomes constant at $t \sim 90$ min (experiments 1-2-3), $t \sim 150$ min (experiment 4) and $t \sim 65$ min (experiment 5) while L_g increases slightly from $t \sim 250$ -280 min (experiments 1-2), $t \sim 210$ min and ~ 170 min (experiments 3 and 4) and $t \sim 530$ min (experiment 5) till the end of the experiment.

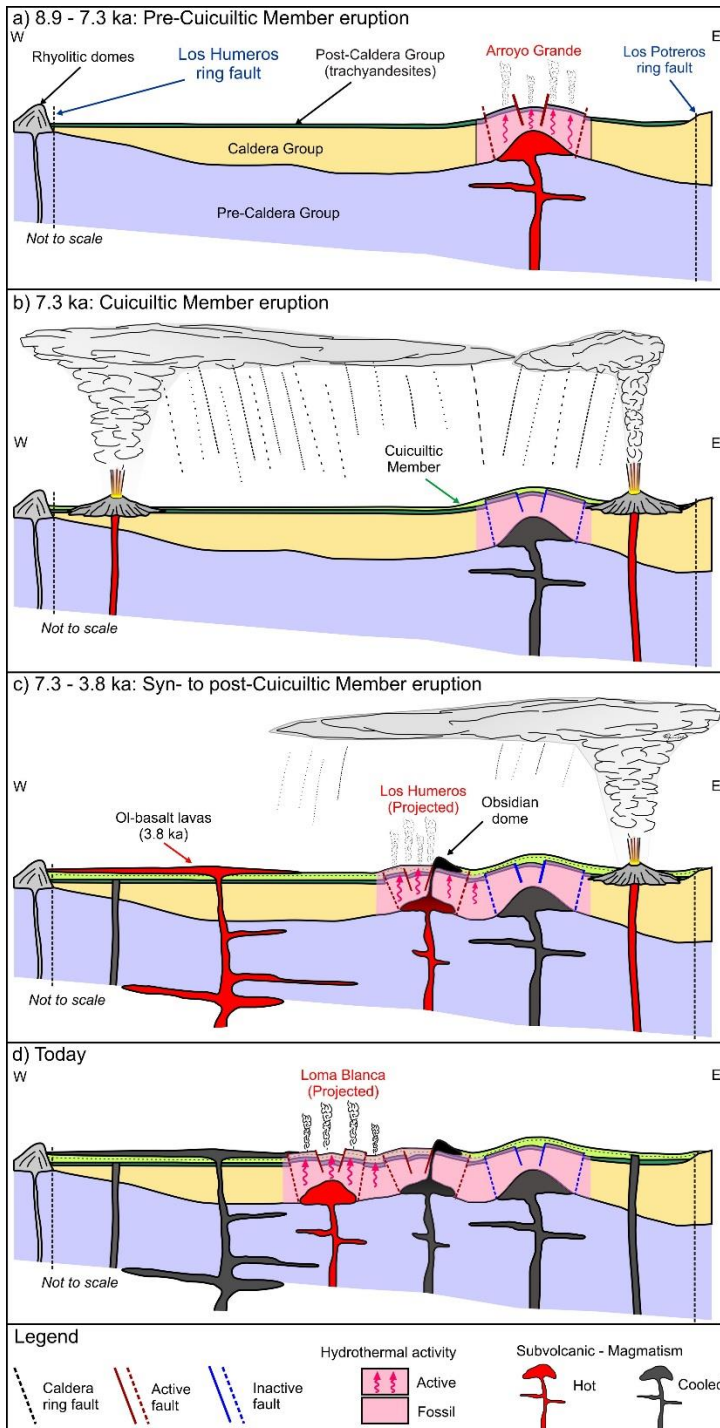


Figure 10: Schematic model of the evolution of the sub-surface structure of the Los Potreros caldera floor. Multiple magmatic intrusions located at relatively shallow depth (< 1 km) are responsible for the localized bulging of the caldera floor (Loma Blanca, Los Humeros and Arroyo Grande uplifted areas). a) Pre Cuicuiltic Member eruption: emplacement of a felsic intrusion at shallow depth and formation of the Arroyo grande bulge characterized by extensional faulting at its top, reverse faulting at its base and hydrothermalism. b) Cuicuiltic Member eruption: eruption of the Cuicuiltic Member covering the hydrothermally altered post-caldera trachyandesitic lavas. c) Syn to post Cuicuiltic Member eruption: formation of the Los Humeros fault and extrusion of obsidian lava domes along the fault scarp. As the trachyandesitic domes are covered with Cuicuiltic Member only at his base, the lava extrusion occurred during and post the Cuicuiltic Member eruption. d) Formation of the Loma Blanca bulge with the current hydrothermal activity and extensional faulting occurring within the apical depression. Notice that the emplacement of the successive most recent domes (Los Humeros and Loma blanca) are not aligned on the same plane, they are shown for practical purposes.

Stage	Age (ka)	Main stratigraphic units
Post-caldera	< 69	Cuicuiltic Member and trachyandesitic to basaltic lavas
		Llano Tuff
		Xoxoctic Tuff
		Rhyolitic domes
Caldera	164-69	Zaragoza ignimbrite
		Faby Tuff
		Xaltipan ignimbrite
Pre-Caldera	700-164	Rhyolitic Domes

Table 1 Summary of the main stratigraphic units of the three evolutionary stages of the Los Humeros Volcanic complex (Carrasco-Núñez et al., 2017b, 2018).

Parameter	Definition	Value (experiments)	Value (nature)
T	Thickness of the overburden	1-5 X 10 ⁻² m	300-2000 m
L _d	Dome diameter	1-1.6 X 10 ⁻¹ m	2000 m
H	Dome height	1.1-2 X 10⁻² m	100 m
ρ _s	Density of brittle overburden	1400 kg/m ³	2800 kg/m³
φ	Angle of internal friction	35°	25-40°
τ ₀	Cohesion (brittle overburden)	300 Pa	10⁶ Pa
ρ _m	Density of intrusive material	1000 kg/m ³	2500 kg/m³
μ _m	Viscosity of intrusive material	10 ⁴ Pa s	10¹⁵ Pa s
g	Gravity	9.8 m/s ²	9.8 m/s²
t	Timespan for deformation	2.8-6.5 X 10 ⁴ s	1.9 X 10¹² s

Table 2. Comparison of the geometric and material properties parameters of the experiments and nature.

Dimensionless ratio	Experiments	Nature
Π ₁ = T/L _d	0.1-0.5	0.15-1
Π ₂ = H/L _d	0.08-0.2	0.05-0.1
Π ₃ = ρ _s /ρ _m	1.4	1.12
Π ₄ = φ	35	25-40
Π ₅ = ρ _m H ² /μ _m t	6.1 X 10 ⁻¹⁰	1.3 X 10⁻²⁰
Π ₆ = ρ _m gHt/μ _m	1.3 X 10 ³	4.6 X 10³
Π ₇ = ρ _s gT/τ ₀	2.3	8.24

Table 3. Definition and values of the dimensionless ratios Π in nature and in the experiments.

Exp	T (mm)	L _g (mm)	L _d (mm)	θ	α	T _t (mm)	σ (%)
1	10	16	116	58°	14°	15.5	55
2	10	14	105	63°	27°	15.4	54
3	30	42	150	58°	14°	37.7	27
4	30	48	138	56°	18°	41.2	37
5	50	58	164	58°	21°	53.7	7

Table 4. Measured (L_g, L_d, θ, α) and imposed (T) parameters in the experiments. T=overburden thickness; L_d= dome diameter; L_g= **apical depression** width; θ= **apical depression** fault dip; α= dome flank mean dip; T_t= theoretical overburden thickness calculated with equation 1 (Brothelande and Merle, 2015, see discussion section); σ= percentage difference between T and T_t.